

Trends in the design of nerve guidance channels in peripheral nerve tissue engineering

*Original*

Trends in the design of nerve guidance channels in peripheral nerve tissue engineering / Chiono, Valeria; TONDA TURO, Chiara. - In: PROGRESS IN NEUROBIOLOGY. - ISSN 0301-0082. - 131:(2015), pp. 87-104. [10.1016/j.pneurobio.2015.06.001]

*Availability:*

This version is available at: 11583/2615670 since: 2021-04-07T13:23:59Z

*Publisher:*

Elsevier

*Published*

DOI:10.1016/j.pneurobio.2015.06.001

*Terms of use:*

This article is made available under terms and conditions as specified in the corresponding bibliographic description in the repository

*Publisher copyright*

Elsevier postprint/Author's Accepted Manuscript

© 2015. This manuscript version is made available under the CC-BY-NC-ND 4.0 license  
<http://creativecommons.org/licenses/by-nc-nd/4.0/>. The final authenticated version is available online at:  
<http://dx.doi.org/10.1016/j.pneurobio.2015.06.001>

(Article begins on next page)

1 **Trends in the design of nerve guidance channels in peripheral nerve tissue**  
2 **engineering**

3

4

5 Valeria Chiono, Chiara Tonda-Turo\*

6

7 [\*] Dr. Chiara Tonda-Turo

8 Department of Mechanical and Aerospace Engineering

9 Politecnico di Torino

10 Corso Duca degli Abruzzi 24, Turin, Italy

11 telephone number: 0039 0903395

12 fax number: 0039 0906999

13 e-mail address: [chiara.tondaturo@polito.it](mailto:chiara.tondaturo@polito.it)

14

15 Valeria Chiono

16 Department of Mechanical and Aerospace Engineering

17 Politecnico di Torino

18 Corso Duca degli Abruzzi 24, Turin, Italy

19

20

1 **Abstract**

2 The current trend of peripheral nerve tissue engineering is the design of advanced nerve guidance  
3 channels (NGCs) acting as physical guidance for regeneration of nerves across lesions. NGCs  
4 should present multifunctional properties aiming to direct the sprouting of axons from the proximal  
5 nerve end, to concentrate growth factors secreted by the injured nerve ends, and to reduce the  
6 ingrowth of scar tissue into the injury site. A critical aspect in the design of NGCs is conferring  
7 them the ability to provide topographic, chemotactic and haptotactic cues that lead to functional  
8 nerve regeneration thus increasing the axon growth rate and avoiding or minimizing end-organ (e.g.  
9 muscle) atrophy. The present work reviews the recent state of the art in NGCs engineering and  
10 defines the external guide and internal fillers structural and compositional requirements that should  
11 be satisfied to improve nerve regeneration, especially in the case of large gaps (> 2cm). Techniques  
12 for NGCs fabrication were described highlighting the innovative approaches direct to enhance the  
13 regeneration of axon stumps compared to current clinical treatments. Furthermore, the possibility to  
14 apply stem cells as internal cues to the NGCs was discussed focusing on scaffold properties  
15 necessary to ensure cell survival. Finally, the optimized features for NGCs design were summarized  
16 showing as multifunctional cues are needed to produce NGCs having improved results in clinics.

17

18 **Table of contents**

19 1. Introduction

20 1.1 Nerve injury

21 1.2 Nerve regeneration process

22 1.3 Current clinical approaches for treating peripheral nerve injuries

23 1.4 Tissue Engineering strategies for peripheral nerve regeneration

24 1.5 Evaluation of NGC biological performance

25 2. Morphology of nerve guidance channels

26 3. Methods for the fabrication of porous conduits and luminal fillers

27 3.1 Conventional techniques

28 3.1.1 Electrospinning

29 3.1.2 Porogen leaching techniques

1 3.1.3 Freeze drying  
2 3.1.4 Non-solvent induced phase separation (NIPS) and thermally induced phase separation (TIPS)  
3 3.1.5 Injectable hydrogels as fillers  
4 3.1.6 Cell-based therapies for axon regrowth  
5 3.2 Rapid prototyping techniques  
6 4. Design trends  
7 5. Conclusions

8

9 **1. Introduction**

10 *1.1 Nerve injury*

11 Peripheral nerves are commonly exposed to physical injuries, usually caused by transportation and  
12 construction accidents, natural disaster and war damage, and other traumas, including iatrogenic  
13 side effects of surgery. Peripheral nerve injuries affect 2.8% of trauma patients, frequently leading  
14 to life-long disability (Wiberg and Terenghi, 2003). The incidence of nerve injuries is relatively  
15 high all over the world. In US over 200,000 peripheral nerve repair procedures are performed  
16 annually (Ichihara et al., 2008). Around 5% of wounds in the extremities can be associated with  
17 peripheral nerve injuries (Huang and Huang, 2006). In contrast with central nervous system (CNS),  
18 peripheral nervous system (PNS) has the intrinsic capacity to regenerate at a certain extent after  
19 injury (Meek et al., 2002; Schmidt and Leach, 2003).

20 Nerve injuries were classified by Sunderland in five grades depending on the severity degree  
21 (Sunderland, 1951). Neurapraxia (grade 1) is related to a block in the fibre conduction; axonotmesis  
22 (grade 2) is associated to axon transection with an intact endoneurium; neurotmesis/neurotmesis +/  
23 neurotmesis ++ (grade 3/ grade 4/ grade 5) range from transaction with intact perineurium to a  
24 completely interrupted nerve. Spontaneous regeneration is influenced by the severity of the injury  
25 and occurs in axonotmesis with a regeneration rate of 1–3 mm/day, resulting in functional recovery  
26 within few weeks for injury around 1 cm. In case of severe injuries, when the nerve trunk has been  
27 completely interrupted (neurotmesis) and the missing gap is large (higher than 2 cm) the  
28 spontaneous regeneration cannot be achieved.

## 1 *1.2 Nerve regeneration process*

2 The regeneration process starts immediately after injury and is based on three different phases  
3 (Deumens et al., 2010). The early phase (1-5 days) is characterized by axon and myelin  
4 degeneration that occurs at distal and proximal sites (Wallerian degeneration). At the same time, the  
5 nucleus of injured neurons adopts an eccentric position within the cell body and the nucleolus  
6 becomes more prominent; neuronal biochemistry and function are altered with an increase of  
7 protein synthesis required for axonal sprouting and growth. During the intermediate phase (from 5  
8 days to weeks), macrophages infiltrate at the injured site contributing to cellular and tissue debris  
9 removal, Schwann cells (SCs) start a robust proliferation due to the lost contact with axons and  
10 proximal stumps develop regenerative axonal sprouts. The newly generated SCs, together with pre-  
11 existing SCs that survived the nerve injury, form the bands of Büngner. The bands of Büngner in  
12 the distal nerve segment are highly aligned tubes formed by basal lamina secreted by SCs. The  
13 topographical property of these bands is crucial for the directional guidance of axon growth, as the  
14 growth cones of sprouting axons use bands of Büngner as a regenerative substrate. In the last phase  
15 of the regeneration process (from weeks to months), the growth cone of sprouting axons extend  
16 within bands of Büngner at a rate of 1-3 mm/day resulting in complete axon regeneration and  
17 functional recovery.

18 The described spontaneous regeneration process occurs in axonotmesis while can be compromised  
19 in neurotmesis where endoneurial tubes are damaged. In these cases, SCs and fibroblasts proliferate  
20 and re-organize in the attempt to re-establish a connective bridge across the lesion, while distal  
21 stumps release chemotactic cues to attract axon sprouts. The spontaneous regeneration process often  
22 fails resulting in abnormal sprouting and neuroma formation. In neurotmesis, reconstructive surgery  
23 is required to achieve anatomical and functional regeneration, exploiting the knowledge of clinical  
24 and translational neurosciences (Wiberg and Terenghi, 2003).

25

26

### 1 *1.3 Current clinical approaches for treating peripheral nerve injuries*

2 End-to-end suturing (nerve coaptation) is the preferred strategy for peripheral nerve regeneration  
3 (A.B. Sanghvi, 2004) and can be applied to repair short nerve gaps. However, when nerve gap is  
4 large and end-to-end reconnection of transected nerve stumps cannot be performed without exerting  
5 tension, a bridging nerve device is necessary (Ichihara et al., 2009). Autograft, i.e. the implantation  
6 of a portion of an autologous nerve, is the preferred clinical strategy for the treatment of peripheral  
7 nerve injuries, as the biomimetic properties of the implanted conduit favor regeneration (Dellon and  
8 Mackinnon, 1988). Drawbacks of this clinical approach include: the possible mismatch between the  
9 diameter of the injured nerve and the autograft, the lack of an adequate amount of autologous nerve  
10 tissue for implantation, neuroma formation at the donor site and the necessity of at least two  
11 surgeries at injured site and at donor site with consequent donor site morbidity and relevant sanitary  
12 costs (Schmidt and Leach, 2003). Beside the above disadvantages, only 40-50% of patients  
13 receiving autografts achieve a successful degree of functional recovery (Lee and Wolfe, 2000). For  
14 this reason, new alternative strategies for peripheral nerve regeneration are under study and  
15 development.

16 Muscle-in-vein conduits have been proposed as an efficient strategy for peripheral nerve  
17 regeneration, making use of autologous tissues (Battiston et al., 2009; Brunelli et al., 1993). The  
18 technique consists of the implantation of a guide based on a vein, filled with skeletal muscle tissue  
19 providing haptotactic and chemotactic cues to the regenerating axons. Although surgeons can apply  
20 this treatment by a single surgery, drawbacks are associated with the use of autologous tissue,  
21 including the healing from multiple injuries and the lack of an adequate amount of autologous tissue  
22 for the treatment of severe nerve injuries.

23 Concerning artificial grafts, several bioresorbable NGCs have been approved by US Food and Drug  
24 Administration for human uses, based on type I collagen (Neuragen®, Neuroflex™,  
25 NeuroMatrix™, NeuraWrap™, NeuroMend™), porcine small intestinal submucosa (Surgis®  
26 Nerve Cuff), poly(glycolic acid) (Neurotube®) and poly(D,L lactide-co-ε-caprolactone)

1 (Neurolac®). However, they are not recommended for larger gaps than 3 cm (Kehoe et al., 2012)  
2 and their biological performances are inferior to autograft that remains the gold standard treatment  
3 for bridging approaches.

4

#### 5 *1.4 Tissue Engineering strategies for peripheral nerve regeneration*

6 Large gaps need alternative clinical solutions to autologous approaches, improving recovery rates  
7 and functional outcome. Current research is focused on the development of engineered “nerve  
8 guides” or “nerve guidance channels” (NGCs) that physically guide regeneration of nerves across  
9 lesions, directing the sprouting of axons from the proximal nerve end, concentrating growth factors  
10 secreted by the injured nerve ends, and reducing the ingrowth of scar tissue into the injury site  
11 (Taras and Jacoby, 2008). Up to now, a wide range of natural or synthetic biomaterials, together  
12 with well-defined fabrication techniques, have been used to prepare NGCs with different structural  
13 and physicochemical properties (Chiono et al., 2009a; Ciardelli and Chiono, 2006; Johnson and  
14 Soucacos, 2008).

15 Biological and physicochemical requirements, such as biocompatibility, biodegradability, adequate  
16 mechanical properties and permeability may be achieved by properly tailoring NGC chemical  
17 composition and structure. Biocompatibility refers to the ability of NGCs to promote appropriate  
18 cellular behaviors, providing molecular and mechanical signaling for nerve regeneration, without  
19 eliciting undesirable effects on neural cells and tissues and/or inducing any undesirable local or  
20 systemic host response.

21 Moreover, an ideal NGC should gradually degrade in vivo as the injured nerve regenerates. For this  
22 reason, degradable and resorbable materials are generally used to prepare nerve conduits. NGCs  
23 should degrade at an appropriate rate which allows the device to withstand the mechanical  
24 compression stresses of surrounding tissues till complete nerve regeneration, avoiding guide  
25 collapse. In addition, degradation should occur with minimal swelling and foreign body reaction (de  
26 Ruyter et al., 2009). Porous guides have been reported to have a decreased degradation rate

1 compared to not porous guides in the case of bulk degradation phenomena, as porosity decreases  
 2 autocatalysis effects (Yucel et al., 2010). On the other hand, surface erosion rate is higher in the  
 3 case of porous guides respect to not porous counterparts since the degradation rate is driven by free  
 4 surface in contact with aqueous solution (Gopferich, 1996). Mechanical properties of nerve guides  
 5 should approach the ones of natural nerves to withstand physiological loads: NGCs should bend  
 6 without kinking and possess a moderate hardness to avoid guide dislocation. Mechanical properties  
 7 of nerves are reference mechanical properties for nerve guides applications (**Table 1**).

8 **Table 1. Mechanical properties for natural nerves reported in scientific literature.**

<b>Nerve type</b>	<b>Elastic modulus (E), MPa</b>	<b>Ultimate tensile strength (UTS), MPa</b>	<b>Elongation at break (<math>\epsilon</math>), mm·mm<sup>-1</sup></b>	<b>Ref.</b>
Mouse sciatic nerve	7	-	-	(Wong et al., 2004)
Rabbit tibial nerve	-	11.7 ±0.7	0.385±0.002	(Nectow et al., 2012)
Rat fresh sciatic nerve	0.580±0.150	2.720±0.970	0.810±0.114	(Borschel et al., 2003)
Rat acellular sciatic nerve	0.576±0.160	1.400±0.290	0.480±0.117	(Borschel et al., 2003)
Intact human nerve	15.87 ± 2.21	6.78±0.57	0.61±0.02	(Dumont and Born, 2005)
Extracted Human nerve	8.19 ± 7.27	8.54± 3.37	1.64 ±0.34	(Dumont and Born, 2005)

9  
 10 Mechanical properties of NGCs depend on the structure of the material, porosity, wall thickness and  
 11 presence of lumen fillers.

12 NGC wall permeability should allow the supply of nutrients and oxygen to cells, following device  
 13 implantation (Gu et al., 2011) and limit the loss of the neurotrophic factors secreted by SCs at the  
 14 distal stump. NGC wall permeability is affected by the chemical composition of the polymer(s)  
 15 constituting the guide (hydrophilic/hydrophobic properties; presence of functional moieties able to  
 16 interact with diffusing molecules), crystallinity degree, wall thickness, porosity degree and pore  
 17 size. Porosity degree has been reported to be the main factor affecting permeability when using



1 hydrophobic material-based NGCs, whereas pore size can be tailored to allow vascularisation and to  
2 hinder fibroblast infiltration, as well as to limit growth factor outward diffusion (Kokai et al., 2009).  
3 The basic structure of a NGC consists of a tubular device with a single lumen, providing the basic  
4 functions of a bridging device for nerve regeneration: isolation of the regenerating axons from scar  
5 tissue, protection of the regenerating nerve against compression by the surrounding tissue,  
6 longitudinal directional guide of regenerating tissue and concentration of the growth factors  
7 secreted by SCs in the end stump.

8 More complex guide designs are available (Daly et al., 2012; Gu et al., 2011) (**Figure 1**), including:

9 i) Single hollow lumen porous or not porous NGCs providing longitudinally oriented grooves  
10 in their lumen surface (Gopferich, 1996) or functionalized with bioactive molecules, such as  
11 adhesion proteins (Chiono et al., 2008a), bioactive peptides (e.g. laminin-derived peptides such as  
12 YIGSR and IKVAV (Chiono et al., 2009a)) enhancing SCs attachment, proliferation and migration  
13 or neurotrophic factors promoting axon growth (Xu et al., 2011). Single hollow lumen NGCs may  
14 lead to not complete reinnervation, due to axon dispersion or polyinnervation of different targets by  
15 the axons of the same motoneuron. Single hollow lumen NGCs are thus recommended for small  
16 lesions (< 30 mm) in the sensory nerves.

17 ii) Porous or not porous single lumen NGCs, containing fillers as topographical cues enhancing  
18 regeneration, mimicking the endoneurial-like structure of autologous nerve grafts. Fillers may  
19 include longitudinally aligned fibers (Matsumoto et al., 2000; Wang et al., 2005), porous sponges  
20 (Tonda-Turo et al., 2011a) or gels (Ceballos et al., 1999; Nakayama et al., 2007) mimicking the  
21 composition and morphology of ECM protein-based intraluminal matrix that naturally supports and  
22 enhances the nerve regeneration (Deumens et al., 2010; Gu et al., 2011). Fillers can be  
23 functionalized with specific peptides/proteins or neurotrophic factors, as described in recent works  
24 (Gu et al., 2011; Jiang et al., 2010; Marquardt and Sakiyama-Elbert, 2013).

25 iii) Multichannel NGCs mimicking the natural compartment structure of nerves (He et al., 2009;  
26 Sun et al., 2012; Sundback et al., 2003). Multichannel NGCs reduce axon dispersion and offer

1 superior surface area for functionalization and cell adhesion and migration as compared to single  
2 lumen NGCs. However, multichannel NGC design reduces permeability and mechanical flexibility.  
3 As a result, multichannel NGCs were found not to induce significant functional improvements as  
4 compared to single lumen NGCs (de Ruiter et al., 2008).

5 The aim of this work is that to analyze the recent trends in the design of NGCs, with a focus on the  
6 role of the NGC architecture to derive guidelines for optimal NGC fabrication.

7

### 8 *1.5 Evaluation of NGC biological performances*

9 The evaluation of NGC biological performances has been investigated in a wide range of  
10 experimental settings both in vitro and in vivo. In vitro cell tests evaluating vitality, adhesion and  
11 proliferation of glial cells (both primary and line cells) are useful to investigate cell response in the  
12 first stage of the regeneration process (Tonda-Turo et al., 2011a; Tonda-Turo et al., 2013). Dorsal  
13 root ganglia and neurons are mainly applied to measure the induction of axon growth and sprouting  
14 (Gnavi et al., 2014). Furthermore, neural stem cells have been used to study the correlation between  
15 NGC features and cell differentiation (Gu et al., 2011; Wang et al., 2012) .A variety of animal  
16 models (rats, rabbits, cats and dogs), nerve gap lengths and anatomical sites (sciatic or median  
17 nerves) have been used to evaluate the performance of NGCs in peripheral nerve regeneration.  
18 Furthermore, a large number of assays for assessing the quality of regeneration have been adopted  
19 by independent laboratories making difficult to compare the results (Yannas et al., 2007). In  
20 general, histological analysis and evaluation of functional recovery are necessary to evaluate the  
21 degree of nerve regeneration (Nichols et al., 2005). Functional analysis offers the most direct  
22 approach for demonstrating that the regenerated nerve has recovered its motor and sensory function  
23 and has correctly innervated the target tissue. Nichols et al. (Nichols et al., 2005) have compiled and  
24 tabulated the available motor tests and observational methods applicable to various models of rat  
25 nerve injury for studying reinnervation in terms of degree and quality of motor and sensory  
26 recovery. In this endeavor, the standardization of experimental conditions and assays could improve

1 any evaluation of peripheral nerve regeneration. Yannas et al. (Yannas et al., 2007) have reviewed  
2 and compared various materials and models for peripheral nerve regeneration concluding that the  
3 quality of regeneration can be maximized addressing two critical aspects: (i) the presence of  
4 fibroblasts surrounding the NGC and infiltrating within the conduit should be minimized; (ii) the  
5 proliferation of SCs and the formation of bands of Bungner serving as tracks for axon elongation  
6 should be encouraged.

7 Experimental models which more closely mimic the environmental and patient clinical conditions  
8 will become a fundamental instrument to enlarge the knowledge in the biochemical mechanisms  
9 involved in the regeneration process.

10

## 11 **2. Morphology of nerve guidance channels**

12 A critical aspect in the design of NGC is conferring them the ability to deliver oxygen and nutrients  
13 to the regenerating nerve tissues to ensure SCs vitality, especially in the case of large gaps (> 2cm)  
14 requiring relatively high recovery times. The first biomaterial based approach to reconnect damaged  
15 nerve stumps employed not porous poly(dimethyl siloxane) (PDMS) tubes: these guides were not  
16 permeable and their only function was that to avoid the risk of scar tissue ingrowth showing a low  
17 axons regeneration and myelination (Jenq and Coggeshall, 1985). Further studies confirmed the  
18 fundamental role of guide permeability to oxygen and nutrient in peripheral nerve regeneration  
19 (Jiang et al., 2010; Lu et al., 2009). To maximize the influx of oxygen and nutrient from the  
20 interstitial fluid, porous guides have to be used, with proper pore size and porosity degree.  
21 Moreover, peripheral nerves are known to be highly vascularized by vasa nervorum along the axon  
22 trunk. Nerve trunk (axon bundles) are supplied by blood by arteriae nervorum. Therefore, nerve  
23 vasculature is fundamental for nerve regeneration. The need for an adequate wall porosity is  
24 contrasted by the opposite need to prevent the infiltration of scar tissue into the NGC lumen and to  
25 minimize the outward diffusion of growth factors, secreted by nerve ends. Tube wall pores should  
26 be interconnected and with suitable size to allow small molecules permeation; on the other hand

1 pore size greater than 20  $\mu\text{m}$  causes fibroblast infiltration as reported by Sarazin et al. (Sarazin et  
2 al., 2004) and should be avoided. Therefore, optimal pore size for external guide should be  
3 comprised in 5-30  $\mu\text{m}$  range and preferable at 10-20  $\mu\text{m}$  range (Dodla and Bellamkonda, 2008;  
4 Jiang et al., 2010; Pfister et al., 2007a; Rodriguez et al., 1999; Vleggeert-Lankamp et al., 2007),  
5 avoiding growth factors outflow and fibroblast infiltration, although allowing nutrient and  
6 catabolyte exchange and endothelial cell migration (vascularization).

7 In addition, nutrient and oxygen inflow increase with decreasing NGC wall thickness. However,  
8 any increase in both NGC porosity (Bian et al., 2009; Yucel et al., 2010) and decrease in the wall  
9 thickness reduce the guide mechanical properties, which can compromise NGC ability to face  
10 compression stresses.

11 Therefore, the morphological properties of the guide (wall thickness, porosity degree, pore size)  
12 have to be carefully designed to satisfy the NGC requirements in terms of mechanical performance  
13 and permeability. To this aim, several conventional and not conventional techniques have been used  
14 to obtain porous NGCs with different structural features. Although optimal NGC structural  
15 parameters also depend on the guide chemical composition (affecting material mechanical  
16 properties), a state-of-the-art analysis of porous NGCs allows the definition of suitable ranges for  
17 guide wall thickness, porosity degree and pore size. In the following sections, the main available  
18 techniques for the fabrication of porous guides will be reviewed deriving the ranges for optimal  
19 NGC structural parameters.

20 Additionally, in the case of large nerve gap ( $> 2$  cm), a porous inner NGC filler may provide  
21 contact guidance for SCs attachment and migration, thus favoring nerve regeneration. The design of  
22 inner fillers should consider the needs for a suitable surface composition allowing cell attachment,  
23 an adequate porosity for cell migration, the additional possibility to deliver neurotrophic factors to  
24 stimulate neuronal outgrowth and a degradation time depending on nerve tissue regeneration rate  
25 (which in turn depends on gap size) (Chen et al., 2006; Jin et al., 2013). Biomimetic 3D structures  
26 able to reproduce the native structure and size of ECM have been reported to strongly influence the

1 cell behavior. Interestingly, these biomimetic structures enhance the nerve regeneration process by  
2 providing synergistic contact guidance for cell adhesion and topographical cues to direct stem cell  
3 fate (Georgiou et al., 2015; Jiang et al., 2012; Lim et al., 2010; Prabhakaran et al., 2009)

4 In the next paragraphs, a state-of-the art analysis of the most successful luminal NGC fillers will be  
5 provided to derive requirements for the design of optimal NGC fillers, in terms of structural,  
6 morphological and physicochemical properties.

7

### 8 **3. Methods for the fabrication of porous conduits and luminal fillers**

9 Conventional and rapid prototyping techniques have been used to prepare porous external conduits  
10 and inner fillers for NGCs. Main conventional techniques used in the field of peripheral nerve tissue  
11 engineering include electrospinning, porogen-leaching, freeze-drying and solvent- or thermally-  
12 induced phase separation. On the other hand, rapid prototyping techniques are a family of emerging  
13 software-driven procedures allowing the controlled layer-by-layer fabrication of scaffolds, which  
14 have been marginally used in the field of peripheral nerve regeneration up to now.

15

#### 16 *3.1 Conventional techniques*

##### 17 *3.1.1 Electrospinning*

18 Electrospinning allows the fabrication of randomly or longitudinally aligned nanofibrous substrates  
19 with fibre diameters ranging from tens of nanometers to several microns. An electric voltage ( $\pm$   
20 5÷50 kV) is applied between a collector and a metal capillary needle from which the polymer  
21 solution or melt is extruded. The applied electric field induces a surface charge on the polymer  
22 solution or melt and the formation of a Taylor cone polymer droplet at the tip of the spinneret. At an  
23 electrical potential exceeding a critical value, electrostatic forces overcome surface tension and a  
24 polymeric jet stream between the capillary needle and the collector forms. Solvent evaporation (in  
25 the case of polymer solutions) or cooling (in the case of polymer melts) occur before nanofibers  
26 reach the collector. Electrospun scaffolds have gained increased interest as they have a similar

1 morphology compared to native ECM (Sill and von Recum, 2008). In addition, electrospinning  
2 allows the obtainment of porous polymer substrates with varying porosity degree and mechanical  
3 properties, having a high surface to volume ratio, enhancing cell-substrate interactions. Porous  
4 guides have been fabricated by electrospinning, having pores with 1-10  $\mu\text{m}$  size, which avoid the  
5 infiltration of fibrous tissue into the NGCs, but allow the ingrowth of endothelial cells  
6 (vascularisation) when pores have higher size than 5 $\mu\text{m}$  (Dodla and Bellamkonda, 2008; Pfister et  
7 al., 2007a; Rodriguez et al., 1999). By changing the collector geometry, substrates with different  
8 structural and morphological features can be prepared, such as flat membranes (which can be  
9 wrapped into tubular guides or cut into stripes used as NGC fillers), mono-layered or bi-layered  
10 hollow tubular structures and fiber mats used as inner fillers. **Table 2** collects significant examples  
11 of potential use of electrospinning technique in the preparation of NGCs. Exhaustive examples are  
12 provided in previous reviews on the use of electrospinning technique for peripheral nerve  
13 regeneration (Xie et al., 2010).

14

1 **Table 2. Use of electrospinning technique in the field of peripheral nerve regeneration.**

Application	Final geometry	Collector type	Product characteristics	Ref.
Hollow guide	Membrane to be wrapped and longitudinal sutured/glued	Grid/plate	Material: copolymer of caprolactone and ethyl ethylene phosphate	(Chew et al., 2007)
	Tube consisting of randomly oriented nanofibres.	Rotating mandrel (with diameter size equal to inner tube size)	Material: blend of poly(L-lactide- <i>co</i> -glycolide) and poly- $\epsilon$ -caprolactone (PLGA/PCL) Pore size: from 700 nm to 20 $\mu$ m	(Panseri et al., 2008)
			Material: PLGA Average pore size: 1 $\mu$ m	(Bini et al., 2004)
	Tube consisting of nanofibres arranged perpendicularly respect to the tube axis.	Rotating mandrel (with diameter size equal to inner tube size)	Material: PCL	(Teo et al., 2005)
	Tube consisting of longitudinally aligned fibres.	Two steel blades (aligned with a gap in between): fibres are deposited along the gap.	Material: PCL	(Teo and Ramakrishna, 2005)
	Double layered tubes with the luminal layer having longitudinally aligned nanofibres and the outer layer based on randomly aligned fibres .	Rotating mandrel (with diameter size equal to inner tube size)	Material: poly (L-lactide- <i>co</i> -caprolactone), poly(propylene glycol) and sodium acetate	(Zhu et al., 2011)
Random fillers	Cut stripes of membranes with randomly oriented nanofibres	Plate or grid	Material: blend of collagen and glycosaminoglycan Porosity degree: 80.68%	(Timnak et al., 2011)
			Material: blend of PLGA and PCL Pore size: $9.9 \pm 2.0 \mu$ m Porosity degree: $64.7 \pm 4.4\%$	(Subramanian et al., 2012)
		Rotating mandrel	Material: chitosan	(Wang et al., 2008)
Directional fillers	Mats of longitudinally aligned fibres used as internal fillers.	Rotating mandrel provided with two insulating segments	Material: blend of PLGA and PCL Pore size: $3.7 \pm 1.7 \mu$ m Porosity degree: $72.0 \pm 13.2 \%$	(Subramanian et al., 2012)
		Two parallel metal rods	Material: blend of polyhydroxybutyrate (PHB) and PLGA	(Yucel et al., 2010)
		Parallel disks (two pole air gap electrospinning system)	Material: PCL Pore size: from 200 nm to 1.8 $\mu$ m. Porosity degree from 58% to 95%.	(Jha et al., 2011)

2

1 **Figure 2** reports the scanning electron microscopy (SEM) images of electrospun tubes and bundles  
2 fabricated according to the procedures reported in **Table 2**.

3 As evidenced in **Table 2** electrospun substrates have been proposed as both hollow guides and  
4 internal filler of NGCs.

5 For hollow guides preparation, synthetic polymers have been applied and different set up and  
6 techniques were investigated. Flat fibrous membranes prepared by electrospinning may be wrapped  
7 around the trunked nerve and, then, longitudinally sutured or glued into a tubular guide (Chew et  
8 al., 2007). Alternative methods for preparing porous NGCs are based on the electrospinning of  
9 polymer solutions onto rotating mandrel collectors with proper diameters according to nerve size  
10 (generally 1-2.5 mm) (Bini et al., 2004; Panseri et al., 2008). Finally, advanced procedures have  
11 been developed to prepare NGCs with longitudinally aligned fibres by electrospinning (Teo and  
12 Ramakrishna, 2005). Teo et al. developed a simple method to collect highly aligned nanofibres  
13 using conductive blades placed in line with a gap in between. Nanofibres were collected at the gap  
14 with one end at the tip of one steel blade and the other end at the other tip showing highly ordered  
15 structure. In the case of polymers with lower mechanical properties, electrospun bi-layered guides  
16 have been prepared, with the aim to increase their mechanical performance and structural stability.  
17 Zhu et al. have fabricated hollow bi-layered nanofibrous NGCs, with longitudinally aligned  
18 nanofibres as the inner layer and randomly oriented nanofibres as the outer layer, based on a blend  
19 between poly(L-lactide-co-caprolactone) and poly(propylene glycol) (Zhu et al., 2011). To this  
20 purpose, a stainless steel rotating mandrel partially coated with insulating polymer layers was used.  
21 Longitudinally aligned nanofibres were first deposited between the two adjacent insulating  
22 segments. After complete deposition of the first layer, changes in the electrical field led to the  
23 deposition of randomly aligned nanofibres on the previous layer.

24 The presence of electrospun fibres on NGC wall increases the total surface area available for cell  
25 adhesion and introduces contact guidance to cell ingrowth. In vivo tests on rats having a 1cm nerve  
26 gap suggested that both randomly oriented and aligned electrospun NGC walls play a significant



1 role during the initial or early phase of nerve regeneration due to the presence of an increased  
2 surface area for cell attachment (Bini et al., 2004; Chew et al., 2007; Panseri et al., 2008).  
3 Myelinated axons were found to grow in close proximity of the electrospun fibers during the initial  
4 months post-implantation (Chew et al., 2007; Panseri et al., 2008) having smaller area, fibre  
5 diameter and density compared to normal nerves (Bini et al., 2004). The effect of morphological  
6 and guidance cues were demonstrated on long-term in vivo studies (12 months post-implantation)  
7 where aligned nanofibrous nerve conduits showed superior regeneration than randomly oriented  
8 nanofibrous conduits and a comparable therapeutic effects to autografts (Zhu et al., 2011).

9 The possibility to fabricate NGC internal fillers based on nanofibres was investigated by many  
10 authors as reported in **Table 2**. Randomly oriented nanofibrous mats were studied as NGC internal  
11 fillers to enhance SCs adhesion and proliferation and consequently improve the regeneration  
12 process (Subramanian et al., 2012; Timnak et al., 2011; Wang et al., 2008). Additional directional  
13 cues can be imparted to SCs by orienting the fibres in the direction of axonal regrowth. Aligned  
14 nanofibres were produced by modifying the collector geometry such as using rotating mandrel  
15 (Subramanian et al., 2012) or parallel metal rods (Yucel et al., 2010). More complex geometries  
16 allowed to obtain three dimensional fibres organization as reported by Jha et al. (Jha et al., 2011).

17 Cylindrical bundles of aligned nano- to micro-fibres (from 200 nm to 1.8  $\mu\text{m}$  average cross-  
18 sectional size) may also be prepared using the “air gap electrospinning” method (Jha et al., 2011).  
19 Jha et al. applied this method to prepare PCL fibre bundles. Bundle porosity, calculated by the  
20 liquid intrusion method as a function of the feed polymer solution concentration, increased from  
21 58% to 95% with increasing PCL solution concentration from 10% (w/v) % to 25% (w/v),  
22 respectively. Complete NGCs was obtained by coating the fibrous bundle through electrospaying  
23 of PGA-PLA (50:50) copolymer aiming at reducing inflammatory cell infiltration into the fibre  
24 arrays during in vivo implantation.

25 Compared to empty tubes, NGCs containing both aligned and randomly oriented electrospun fibres  
26 showed to promote SC migration into the lesion area creating a growth permissive environment that

1 enables axons to grow through the lesion site (Timnak et al., 2011; Wang et al., 2008). However,  
2 aligned nanofibres mimicking the anisotropic structure of the native tissue facilitate the formation  
3 of longitudinal columns of SCs resembling the in vivo architecture of endo-neural peripheral nerve  
4 processes (Subramanian et al., 2012). In vivo tests on rats reported that 25% of the axons present in  
5 the proximal section reached the distal stumps in a two-fold reduction time if the NGC presents  
6 PCL aligned nanofibres as internal filler compared to PCL empty tube (Jha et al., 2011).

7 Natural polymers such as proteins (gelatin, collagen and silk fibroin) and polysaccharides (chitosan,  
8 hyaluronic acid and cellulose) showed higher biomimetic properties than synthetic materials but  
9 they are difficult to be electrospun, because of their low solubility in organic solvents, the risk for  
10 protein denaturation (Zeugolis et al., 2008) and high viscosity of polysaccharide solutions  
11 (Homayoni et al., 2009). Natural polymers have been generally electrospun using highly toxic  
12 solvents, such as 2,2,2-trifluoroethanol (Huang et al., 2004), acetic acid (Song et al., 2008),  
13 1,1,1,3,3,3-hexafluoro-2-propanol (Kim et al., 2005) and formic acid (Ki et al., 2005). Electrospun  
14 collagen flat membranes have been prepared by Timnak et al. with randomly oriented or  
15 longitudinally aligned fibers and have been crosslinked by genipin (Timnak et al., 2011). Collagen  
16 solution in 1,1,1,3,3,3-hexafluoro-2-propanol (HFP):Acetic Acid (AAc) (1:1) has been electrospun  
17 into longitudinally aligned fibers, using a rotating cylindrical mandrel at an optimal speed of 2600  
18 rpm. Porosity of membranes composed of randomly oriented fibers was around 80%, whereas that  
19 of membranes with aligned fibers was not quantified. Membranes with aligned fibers showed closer  
20 mechanical properties to those of an intact nerve (**Table 1**) as compared to membranes with  
21 randomly oriented fibers (UTS:  $5.200\pm 0.600$  MPa vs.  $0.60\pm 0.10$  MPa; ultimate strain:  $1.021\pm 0.002$   
22 mm/mm vs.  $1.14\pm 0.03$  mm/mm).

23 As an alternative to the current electrospinning methods employing organic solvents, the authors of  
24 this work have recently fabricated porous glycidoxypropyltrimethoxysilane (GPTMS) crosslinked  
25 gelatin membranes, based on randomly oriented electrospun nanofibers with an average diameter of  
26 300 nm, using water as a solvent (Tonda-Turo et al., 2013). Addition of GPTMS crosslinker into

1 the gelatin solution did not cause any significant increase of solution viscosity during the  
2 electrospinning process, as the condensation reaction involved in GPTMS-mediated crosslinking  
3 occurred only after complete solvent evaporation (i.e. at the collector). The adhesion and  
4 proliferation of glial-like cells on nanofibrous matrices confirmed the potentiality of these scaffolds  
5 as substrates for peripheral nerve tissue engineering. Electrospinning of aqueous solution is  
6 advantageous as it not only avoids the use of cytotoxic organic solvents, but it also preserves  
7 proteins from denaturation. Growth factors may be incorporated into natural polymer nanofibres  
8 prepared from water solutions, without losing their bioactivity.

9 Due to their superior mechanical resistance and peculiar physicochemical properties, such as  
10 limited swelling and unaltered mechanical properties in physiological fluids as well as high  
11 degradation times, synthetic polymers are ideal candidates for the fabrication of NGCs external  
12 conduits. On the contrary, natural polymers have low mechanical resistance, especially in swollen  
13 state, and short degradation times but, as an advantage, they display biomimetic characteristics,  
14 supporting nerve regeneration. For these reasons, they are generally preferred for the preparation of  
15 fillers or inner tube surface coatings for NGCs. Based on these considerations, electrospinning  
16 methods collected in **Table 2** could be ideally applied to prepare porous tubular guides based on  
17 synthetic polymers, internally coated or filled respectively with a layer or a bundle of longitudinally  
18 oriented natural polymer fibres.

19 The main advantages related to electrospinning technique lies in the possibility to mimic the  
20 architecture of natural ECM and fabricate biomimetic structure in an easy manner. Many studies  
21 have demonstrated that nanofibres alone support stem cell culture and induce differentiation into  
22 neural lineage (Jiang et al., 2012; Lim et al., 2010; Prabhakaran et al., 2009).

23

24

25

26

### 1 3.1.2 Porogen leaching techniques

2 Porous tubular guides or inner fillers can be prepared by blending the selected structural polymers  
3 with a second component (porogen), which can be an inorganic compound, such as NaCl or a low-  
4 cost polymer removed by dissolution in a selective solvent.

5 Salt leaching technique has been applied to fabricate NGCs (Kokai et al., 2009). Pore morphology  
6 depends on the salt crystals, while porosity is mainly affected by salt weight fraction (Widmer et al.,  
7 1998). One drawback of this technique is poor pore interconnection. Attainable pore size varies in  
8 the 10-300  $\mu\text{m}$  range (Kokai et al., 2009; Widmer et al., 1998), depending on salt particle size.  
9 However, pore size higher than 30  $\mu\text{m}$  allows fibroblast infiltration and neurotrophic factors  
10 outflow and is suboptimal for NGCs. Kokai et al. prepared NGCs by dip-coating a mandrel with a  
11 NaCl suspension in poly(caprolactone) (PCL) solution, followed by drying and particulate leaching  
12 (Kokai et al., 2009). They found out the following optimal structural parameters for NGCs: 80%  
13 porosity degree, 10-38  $\mu\text{m}$  pore size and 0.6 mm wall thickness. Due to the relatively high pore size  
14 respect to the recommended value (10-20  $\mu\text{m}$ ), wall thickness was increased to limit growth factor  
15 outward diffusion (studied using lysozyme as model molecule), without affecting glucose  
16 permeability (**Figure 3 A-B**).

17 Blending a structural polymer with a porogen polymer offers the possibility to tailor pore size, by  
18 blend composition and processing conditions (Tonda-Turo et al., 2011a; Yucel et al., 2010).  
19 Suitable blend compositions for the fabrication of porous guides according to this method are  
20 generally below the “co-continuity” region, to afford suitable mechanical properties. After the  
21 removal of the leaching polymer component, a not interconnected porosity is thus formed, which  
22 does not allow the convective flux of fluids between the guide lumen and the external environment  
23 in the first period post-implantation. However, the presence of pores may enhance diffusive  
24 exchanges of nutrients and catabolites. In a previous work, Chiono et al. demonstrated that non  
25 porous PCL melt-extruded guides were effective for the repair of small (0.5 cm) and medium (1.5  
26 cm) size nerve defects in the peroneal and median nerve of Wistar rats, respectively (Chiono et al.,

1 2009b). However, PCL guides failed in the regeneration of a 4.5 cm long defect in the median nerve  
2 of Wistar rats in a cross-chest experimental model, due to guide detachment from the implantation  
3 site, caused by guide rigidity. Further efforts were devoted to increase PCL mechanical flexibility  
4 by introducing pores into the tubular conduit wall, which could also increase nutrient diffusion rate  
5 favoring nerve regeneration. To this aim, a simple method was developed and recently published by  
6 the authors (Tonda-Turo et al., 2011a) based on the preparation of PCL/ poly(ethylene oxide) (PEO)  
7 blends by solution mixing, followed by the fabrication of blend tubes by dip-coating/rotating  
8 mandrel technique and final PEO selective dissolution leading to porous guides (**Figure 3 C-D**).  
9 Different PCL/PEO blend compositions were prepared with PEO content from 10 to 50 wt.%.  
10 Porous PCL guides were coded as PCL100i, PCL90i, PCL80i, PCL70i, PCL60i, and PCL50i,  
11 respectively for guides prepared from PCL/PEO 100/0, 90/10, 80/20, 70/30, 60/40 and 50/50  
12 wt./wt. after PEO dissolution. Permeability of PCL porous NGCs was determined using FITC-  
13 labeled dextran with 4400 Da molecular weight (FD-4, Sigma Aldrich). FD-4 was used as a model  
14 molecule to study nutrient diffusion due to its higher Stokes radius (14 Å) compared to glucose (3.8  
15 Å) (Schultz and Solomon, 1961) and NaCl (1.4 Å) (Boyle et al., 1979). Tubes filled with FD-4  
16 solutions were soaked in 10 ml PBS and FD-4 concentration in the incubation medium was assayed  
17 by UV-Vis spectroscopy at different time points. The concentration of released FD-4 in the external  
18 PBS solution was plotted as percentage respect to the initial concentration filling the tube, as a  
19 function of time, for different PCL-based conduits (**Figure 4**). Not-porous PCL NGCs were found  
20 to allow the diffusion of small molecules (FD-4): at short time (3-9 hours), the amount of released  
21 solute was around 20-25%, it reached 40-50% after 24-48 hours, and it was 70% after 5 days (168  
22 hours). The behavior of PCL90i and PCL 80i was similar to that of control PCL guides, whereas  
23 permeability of PCL70i, PCL60i and PCL50i was significantly improved compared to the control  
24 after 9 hours. PCL60i was finally selected for the fabrication of guides as it showed partially  
25 interconnected pores with  $0.90\pm 0.25\mu\text{m}$  size, suitable mechanical properties (Tonda-Turo et al.,  
26 2011a) and optimal permeability to nutrients that guarantee cell survival within the conduits.

1 The authors tested the same technique on an elastomeric poly(ester urethane) (PU), previously  
2 employed to prepare not-porous melt-extruded PU conduits for regeneration of peripheral nerves  
3 (Chiono et al., 2011). In detail, PU/PEO (PEO Mw: 100,000 Da; Sigma-Aldrich) 60/40 wt./wt.  
4 blend was obtained by solution mixing technique preparing a 5% (wt./vol.) solution using  
5 chloroform as solvent. PU/PEO 60/40 tubes were fabricated by dipping a 1.3 mm metal bar into  
6 PU/PEO solution; then, the system was air-dried for 30 min. Dipping and drying steps were  
7 repeated three times. Prepared tubes were finally dried and, then immersed in distilled water for 48h  
8 to dissolve PEO (PU60i). PU60i tubes were analyzed for their morphology evidencing a not-porous  
9 structure (**Figure 3 E-F**). Due to PU elastomeric properties, macromolecular chains rearranged their  
10 conformation after PEO removal resulting in a compact structure instead of a porous one (as  
11 observed for PCL). As a conclusion, PEO leaching technique can be successfully applied to glassy  
12 or semi-crystalline polymers due to the limited mobility of macromolecular chains, whereas it  
13 cannot be applied elastomeric polymers.

14

### 15 *3.1.3 Freeze drying*

16 Freeze-drying is an advantageous technique to prepare porous substrates, as it does not require the  
17 use of porogens. The procedure is simple: initially, water based polymer solutions are prepared,  
18 then they are frozen and, finally, they are freeze-dried for ice sublimation. Natural polymers have  
19 been widely used due to their water solubility and different pore micro-architectures have been  
20 obtained (Stokols and Tuszynski, 2004). Freeze-dried substrates based on natural polymers have  
21 been generally used as porous NGC luminal fillers, showing interconnected pores for cell  
22 infiltration and tissue growth. For instance, an luminal NGC filler based on freeze-dried genipin-  
23 crosslinked gelatin (GL/GP) has been developed by the authors (Tonda-Turo et al., 2011a). The  
24 GL/GP porous matrix showed an interconnected porosity with pores of around 62  $\mu\text{m}$  size, which  
25 were suitable for glial-like cells adhesion and proliferation (**Figure 5A**).

1 By modified freeze-drying approaches, porous matrices with oriented pores have been obtained.  
2 Collagen/heparin sulfate (100/1 wt./wt.) sponge-like fillers with oriented pores were prepared by  
3 freeze-drying a collagen/heparin sulfate solution inserted into a tube with 3 mm inner diameter,  
4 previously immersed in liquid nitrogen at a rate of  $2 \cdot 10^{-5} \text{ m} \cdot \text{s}^{-1}$  (Wang et al., 2012). Scaffold pores  
5 size was comprised between 78 and 109  $\mu\text{m}$  whereas porosity degree was about 89%. Sponges were  
6 found to support the adhesion and proliferation of neural stem cells, which distributed along the  
7 pore direction. The use of heparin sulfate was proposed for the incorporation of heparin-binding  
8 growth factors, such as FGF, stimulating axon regeneration (**Figure 5B**).

9 Bozkurt et al. prepared collagen-based nerve guides (Perimaix) having longitudinally oriented  
10 channels with an average diameter of around  $50\mu\text{m}$ , using a patented unidirectional freezing process  
11 (Bozkurt et al., 2012). The channels were continuous from one end to the other one of the NGC and  
12 stabilized by collagen strands perpendicular to the longitudinal axis. Schwann cells were cultured  
13 within the Perimaix scaffold, which was then implanted for the treatment of a 2 cm long defect in  
14 the rat sciatic nerve. The longitudinally oriented channels supported directional glial cell migration  
15 and histological micrographs confirmed that SCs were aligned in a columnar fashion within the  
16 orientated micro-channels at one week and 6 weeks after implantation. The regenerative properties  
17 of SC-cultured Perimaix NGCs were similar to those of autografts, after 1 and 6 weeks implantation  
18 time. However, future Perimaix strategies should consider the need to develop a tubular component  
19 replacing damaged epineurium (**Figure 5 C-D**).

20 Ao et al. applied an unidirectional temperature gradient to induce uniaxial phase separation to  
21 fabricate aligned channels as internal filler of NGCs (Ao et al., 2006). Multimicrotubule chitosan  
22 conduits (M-conduits) were fabricated starting from a chitosan hollow guide that was inserted into a  
23 properly-dimensional styrofoam pedestal, and filled with chitosan acetic acid solution. Then, the  
24 styrofoam pedestal was rapidly covered with a pre-cooled stainless steel cover plate, and placed in a  
25 freezer ( $-20$  to  $-80^{\circ}\text{C}$ ). Thanks to the presence of the styrofoam pedestal the phase separation  
26 process occurred from the top end to the bottom end of the chitosan solution. The frozen samples

1 were freeze-dried to remove iced solvent and then immersed for 10–20 min into 2% (w/v) sodium  
2 hydroxide (NaOH) solution to neutralize the remaining acetic acid. Oriented microtubules were  
3 formed and their diameter was controlled by adjusting the polymer concentration and the cooling  
4 temperature. In details, microchannel diameter can be reduced by increasing solution concentration  
5 and decreasing freezing temperature. Using a chitosan acetic acid solution with 4% (w/v)  
6 concentration and a freezing temperature of  $-40^{\circ}\text{C}$ , microchannels with hexagonal section were  
7 obtained. Their size ranged from 10 to 150  $\mu\text{m}$  and about 73% of the microchannels showed a  
8 diameter of 30–90  $\mu\text{m}$ . In vitro cell tests were performed using mouse neuroblastoma cell line  
9 (Neuro-2a cells) and confirmed that this multitubular NGC is promising as scaffold for peripheral  
10 nerve regeneration thanks to the presence of a proper porosity for fluid exchange and topographical  
11 cues for SC 3D organization.

12 Although mechanical properties of natural polymers are generally poor to allow their use as  
13 materials for external guides, crosslinking may not only reduce water absorption and degradation  
14 rate but even increase mechanical performance (Tonda-Turo et al., 2011b). In this context, the  
15 authors fabricated porous chitosan (CS, medium molecular weight, 75%-85% deacetylated, Sigma  
16 Aldrich) membranes, by freeze-drying CS solutions in 0.5 M acetic acid with 2.5% wt./vol  
17 concentration. CS substrates display low mechanical strength and undergo significant swelling in  
18 wet state (physiological conditions) which both limit their use as NGC in clinical applications.  
19 Aiming at improving CS membrane mechanical properties and their shape stability in physiological  
20 conditions, the authors studied the effect of a silane agent (GPTMS) used as CS crosslinker.  
21 GPTMS was added to CS solution at 75% wt./wt. concentration with respect to CS (the amount of  
22 GPTMS was optimized to have the maximum crosslinking degree of CS chains). The resulting  
23 solution (CS/GPTMS solution) was kept under stirring at  $50^{\circ}\text{C}$  for 1 hours. The porous membranes  
24 were fabricated by pouring the CS/GPTMS solution (3ml) into 60 mm Petri dishes followed by  
25 freezing at  $-20^{\circ}\text{C}$  for 24 hours. The frozen samples were subsequently freeze-dried at  $-20^{\circ}\text{C}$  for 24  
26 hours. The acetic acid was then neutralized by rinsing in a 0.25 M NaOH solution followed by ten



1 washing steps in distilled water. A second freeze-drying process was carried out to maintain the  
2 membrane porous structure. The membranes were highly porous (**Figure 6**) with interconnected  
3 pores having a mean pore size of  $13.4\pm 9.6\ \mu\text{m}$ . Compressive stress–strain curves for the CS and  
4 CS/GPTMS freeze-dried substrates were measured using cylindrical specimens with 1 cm diameter  
5 and 1 cm height in a MTS QTest/10 device. All the specimens were compressed at an uniform  
6 strain rate of 10 mm/min and the compressive force was applied along the height of the samples.  
7 Three specimens for each kind of material were tested. Young’s modulus (E) and collapse modulus  
8 ( $E^*$ ) were measured from the stress-strain curves (Kanungo et al., 2008). Crosslinked samples  
9 showed increased values of E and  $E^*$  respect to uncrosslinked ones: E and  $E^*$  were  $559.0\pm 51.2\ \text{kPa}$   
10 and  $100.6\pm 13.2\ \text{kPa}$  for CS and  $1012.8\pm 87.8\ \text{kPa}$  and  $116.3\pm 8.2\ \text{kPa}$  for CS/GPTMS. The statistical  
11 significant increase of E and  $E^*$  values for CS/GPTMS samples ( $*p<0.05$ ) was a consequence of  
12 the mechanical reinforcement associated with crosslinking process. Furthermore, qualitative tests  
13 indicated the superior elastic behavior of CS/GPTMS membranes which facilitates wrapping of the  
14 porous membrane without plastic deformation. The crosslinked CS/GPTMS porous membranes are  
15 expected to be easily wrapped around the trunked nerve stumps, allowing their use for the  
16 preparation of NGCs during the surgical intervention, with the more appropriate size depending on  
17 the treated nerve diameter.

18

### 19 *3.1.4 Non-solvent induced phase separation (NIPS) and thermally induced phase separation (TIPS)*

20 Phase separation-based methods convert a homogeneous polymeric solution into a biphasic system  
21 in which the polymer-rich phase constitutes the scaffold matrix, whereas the polymer-poor phase  
22 forms the matrix pores. The phenomenon is driven by inducing a thermodynamic instability through  
23 a change in composition or temperature. Phase separation techniques applied in TE include non-  
24 solvent induced phase separation (NIPS) and thermally induced phase separation (TIPS). In NIPS,  
25 phase separation is caused by the contact of the polymer solution with a non-solvent, leading to  
26 polymer precipitation. In TIPS, a polymer solution is prepared at higher temperature than upper

1 critical solution temperature; then, it is quenched to induce phase separation. The solvent is  
2 eliminated through immersion of the system in a polymer non-solvent.

3 Phase separation techniques has been explored in order to produce NGCs with interconnected  
4 porous structure through one simple process that is scalable, fast and controllable.

5 Oh et al. applied NIPS to prepare asymmetrically porous poly(lactic acid-co-glycolic acid) (PLGA)  
6 NGCs (Oh et al., 2008). An alginate hydrogel rod was immersed into a PLGA solution in glycofurol  
7 and Pluronic F127 was used as hydrophilic additive. Phase inversion was carried out by immersion  
8 in a water bath. Prepared NGCs (diameter of 1.5 mm and wall thickness of 0.4 mm) showed  
9 asymmetric column shaped porous structure, with nanosized pores on the inner tube surface (~50  
10 nm) and microsized pores on the outer tube surface (~50  $\mu\text{m}$ ) (**Figure 7A**). The developed NGCs  
11 were tested in vivo removing 10 mm of sciatic nerve. Immunohistochemical analysis was  
12 performed at 1, 2, 4, and 8 weeks post-implantation while histological evaluation at was carried out  
13 at 12 and 24 weeks post-implantation. Compared to non porous silicone tubes, asymmetrically  
14 porous PLGA tubes showed a faster axonal growth (axons reached the distal stump after about 4  
15 weeks) and larger axon diameter and thicker myelin sheath at 12 and 24 weeks.

16 Hsu et al. combined microprinting and NIPS to obtain poly(D,L-lactic acid) (PLA) substrates to be  
17 rolled into NGCs, exhibiting microgrooves on their inner surface for directional guidance and  
18 asymmetric porosity for providing asymmetric permeability (Hsu and Ni, 2009). PLA solution in  
19 dioxane was cast on a patterned PDMS mold. Then, the samples were immersed in ethyl  
20 alcohol/water solutions with different concentrations (95, 40, 20 vol. %). The average pore size  
21 increased while the groove integrity decreased with decreasing ethyl alcohol concentration.  
22 Asymmetric pores formed when 40 and 20 vol. % ethyl alcohol was used as non-solvent: on the  
23 microgrooved surface, pores showed 5  $\mu\text{m}$  size, while on the unpatterned surface, elliptical pores  
24 were present, with 10  $\mu\text{m}$  x 5  $\mu\text{m}$  and 20  $\mu\text{m}$  x 10  $\mu\text{m}$  size, for samples obtained using 40 vol.% and  
25 20 vol.% ethyl alcohol, respectively. Substrates obtained using 40 vol.% ethyl alcohol showed  
26 directional selectivity in bovine serum albumin (BSA) permeability. Furthermore, in vivo results

1 obtained using the rat sciatic nerve model with 10mm nerve defect showed a higher degree of  
2 myelination at 4 weeks and at 6 weeks in the asymmetric conduits with surface microgrooves than  
3 on asymmetric conduits without surface microgrooves highlighting the importance of wall porosity  
4 on the regeneration process.

5 The authors combined dry-jet-wet spinning technique and NIPS to prepare porous poly(3-  
6 hydroxybutyrate-co-3-hydroxyvalerate)/poly( $\epsilon$ -caprolactone) (PHBHV/PCL) hollow conduits for  
7 biomedical applications (Chiono et al., 2008b). For PHBHV/PCL blends with PCL content  $\leq$  60  
8 wt.%, continuous hollow fibers were obtained with low porosity degree and rough porous inner and  
9 outer surfaces (**Figure 7C**). Pore size was lower than 10  $\mu\text{m}$ . Fibers with the same composition and  
10 tailored size (obtained by properly varying the spinneret size and non solvent flow rate into the  
11 inner cavity) could be potentially exploited for peripheral nerve regeneration.

12 Sun et al. developed a multi-channeled nanofibrous poly(L-lactic acid) (PLLA) NGC through  
13 injection molding and TIPS techniques (Sun et al., 2012) to fabricate a multi-structural guide having  
14 porous external wall and internal microchannels (**Figure 8**). PLLA solutions in tetrahydrofuran with  
15 6-12 % wt. $\cdot$ vol.<sup>-1</sup> concentration were prepared and injected into molds, followed by phase separation  
16 at -80°C for 12 h. Subsequently, the solvent was exchanged with ice-cold distilled water. Resulting  
17 scaffolds were negative replica of the mold characterized by internal microchannels and channels  
18 wall consisted of interconnected nanofibers with 157-161 nm size. Fiber length and scaffold  
19 porosity decreased with increasing PLLA solution concentration from 1250 nm to 556 nm and from  
20 92 to 85%, respectively. The porous nanofibrous channeled matrix was proposed as luminal filler to  
21 guide the regeneration of oriented axon bundles. Preliminary in vitro tests using rat adrenal  
22 pheochromocytoma cell line (PC12 cells) showed an increased cell adhesion on conduits with inner  
23 fillers.

24

25

26

### 1 *3.1.5 Injectable hydrogels as fillers*

2 In peripheral nerve tissue engineering, hydrogels are applied as NGC fillers, serving to physically  
3 bolster the nerve conduit lumen, and to act as delivery vehicles for bioactive molecules and cells  
4 (Lin and Marra, 2012). Tubes filled with fibrin matrices (Williams et al., 1987), laminin containing  
5 gels (Madison et al., 1985), collagen (Ciardelli and Chiono, 2006; Cordeiro et al., 1989), hyaluronic  
6 acid (Seckel et al., 1995) have shown faster axonal regeneration compared to empty tubes or tubes  
7 containing physiological saline solution. Despite many studies demonstrated that NGC fillers can  
8 enhance the regeneration process, hydrogels with unsuitable physicochemical properties could  
9 represent a physical barrier to axonal growth impeding regeneration. Therefore hydrogels to be  
10 applied as internal fillers for NGCs should be designed to have suitable morphological properties  
11 (i.e. to have a proper intrinsic porosity to allow nutrient diffusion) and a degradation rate matching  
12 the nerve regeneration rate to avoid any risk of hindering axon re-growth.

13 Many hydrogel types with different chemical and physical properties have been developed over the  
14 last several decades from a wide variety of materials. In the past, many applications in peripheral  
15 nerve regeneration have made use of synthetic water soluble polymers such as poly(acrylic acids),  
16 poly(acrylamides), poly(ethelene oxide), poly(vinyl alcohols), and poly(vinyl pyrrolidones) (Lyons  
17 et al., 2009; Mahoney and Anseth, 2006; Martens et al., 2003). Synthetic water soluble polymers  
18 are advantageous due to their mechanical properties, processability and chemical reproducibility but  
19 they lack ECM biomimetic properties which are crucial for cell adhesion and proliferation.

20 To improve hydrogel biological response, natural polymers such as hyaluronic acid, fibrin and  
21 chitosan, have been widely used in tissue engineering applications (Balgude et al., 2001; Crompton  
22 et al., 2007; Meena et al., 2007; Sakiyama et al., 1999) as they provide biomimetic chemical and  
23 morphological cues.

24 The use of water soluble hydrogels as NGC fillers allowed the loading of biomolecules and cells  
25 within the hollow guide. Localized growth factor release and cell-based therapy have been recently

1 identified as advanced approaches that can improve the NGC performances and in vivo outcomes to  
2 overlap the gap between biological response of artificial graft compared to autograft.

3 Authors have recently developed a natural origin injectable hydrogel as filler for NGCs (Tonda-  
4 Turo et al., 2014). The developed agar/gelatin (A/GL) hydrogels crosslinked using genipin  
5 (A/GL\_GP) showed shear-thinning behaviour allowing their injection through a syringe needle into  
6 a hollow guide during surgery (**Figure 9**). *In vitro* cellular tests using mouse embryonic fibroblast  
7 cell line (NIH3T3), neonatal olfactory bulb ensheathing cells (NOBECs) and a Schwann cell line  
8 (RT4-D6P2T) confirmed cell adhesion, proliferation and viability. Furthermore, three-dimensional  
9 migration assay confirmed the capability of the developed hydrogel to allow cell migration by a  
10 porous structure that reduces the risk of axonal growth obstruction.

11 The developed hydrogel was studied as a drug delivery system for growth factor localized release.  
12 The mild conditions employed for the preparation of A/GL\_GP hydrogel (low temperature and  
13 physiological pH) could ideally allow the incorporation of growth factors, as chemotactical cues  
14 enhancing the regeneration process (Pfister et al., 2007b). Vascular endothelial growth factor  
15 (VEGF) was added to the hydrogel prior to gelation and VEGF release kinetics and bioactivity after  
16 release were analyzed through ELISA kit and in vitro tests using human umbilical vein endothelial  
17 cells (HUVECs), respectively. Results from in vitro tests showed that GL-based hydrogel system  
18 was suitable for incorporation and release of bioactive VEGF, which could be exploited to induce  
19 capillary-like tube formation and axonal outgrowth (Gnavi et al, 2014). Furthermore, drug release  
20 kinetics could be modulated in multifunctional systems where bioactive agents were loaded in  
21 hollow glass fibers made of resorbable phosphate glass ( $50\text{P}_2\text{O}_5-30\text{CaO}-9\text{Na}_2\text{O}-3\text{SiO}_2-$   
22  $3\text{MgO}-2.5\text{K}_2\text{O}-2.5\text{TiO}_2$  mol%) dispersed in a A/GL\_GP hydrogel (Novajra et al., 2014). Hollow  
23 fibers can be used both as a directional fillers and carriers with high surface area for drug delivery.

24 In addition, thanks to their high water content and their structural similarity to many soft tissues,  
25 hydrogels have been used to encapsulate cells in a three dimensional environment (Suri and  
26 Schmidt, 2010). In this context, hydrogels act as a vehicle for cell-based replacement therapy

1 reducing drawbacks related with transplantation of matrix-free cells (e.g. dislocation, low survival  
2 and poor 3D organisation).

3

#### 4 *3.1.6 Cell-based therapies for axon regrowth*

5 Recently, cell-based therapies have been identified as promising strategies for treatment of injured  
6 peripheral nerve. The presence of transplanted cells is important for the formation of oriented path  
7 for axonal growth and orientation (bands of Büngner) (Galla et al., 2004; Suri and Schmidt, 2010).

8 Galla et al. (Galla et al., 2004) studied the effect of fibrin hydrogels as vehicle for transplanted cells.

9 Schwann cells were inserted into PCL tubes in three different ways: as a non-structured cell  
10 suspension or embedded in a three dimensional matrix containing or not the neurotrophic factor LIF  
11 (leukemia inhibitory factor). In vivo response of the three different systems was evaluated in the

12 repair of a 10 mm gap in the buccal branch of the rat facial nerve. Histological and morphometric  
13 analyses of the implants were performed after four weeks implantation, revealing that three  
14 dimensional fibrin/Schwann cells matrix enhanced the quantity and the quality of peripheral nerve  
15 regeneration through PCL conduits. Furthermore, the presence of LIF prevented hyperneurotization.

16 Hydrogels composed by ECM components, including proteins and glycosaminoglycans, have been  
17 developed as cell-housing devices, in an attempt to recapitulate ECM's structural, biological, and  
18 mechanical properties and to fabricate a biomimetic environment for cell encapsulation. In the

19 native environment, SCs are surrounded by endoneurium, the ECM of neural tissue, which is  
20 composed mainly by hyaluronic acid (HA), collagen IV, and laminin. Therefore, hydrogels for SCs  
21 encapsulation should mimic the neural ECM composition in order to facilitate the cell/scaffold

22 interactions and to enhance cell survival, viability and maintenance of typical glial cell spindle and  
23 star-shape morphology. Suri et al. (Suri and Schmidt, 2010) have designed and tested a collagen and  
24 HA interpenetrating polymer network (IPN) as 3D ECM-mimicking scaffold for SCs encapsulation.

25 Moreover, to further analyze the influence of hydrogel composition on cellular behaviour, laminin  
26 was added to collagen/HA hydrogels. Laminin was selected since it has been reported to enhance

1 the neurite extension and influence SC migration (Thompson and Buettner, 2001). Collagen/HA  
2 hydrogels supported SC viability for 2 weeks and encapsulated cells were able to proliferate and  
3 spread within the gel especially when a high cell density ( $8 \times 10^6$  cells/ml compared to  $2 \times 10^6$  cells/ml)  
4 was loaded into the hydrogel favouring cell-cell interactions. Morphological observations through  
5 SEM reveal that cells were able to remodel the hydrogel by secreting ECM molecules. Finally, the  
6 amount of nerve growth factor (NGF) and brain-derived neurotrophic factor (BDNF) released from  
7 encapsulated SC was quantified to evaluate cellular functional activity. Laminin-containing  
8 hydrogels induced significantly higher NGF and BDNF secretion demonstrating the importance of  
9 hydrogel composition to loaded SC survival and bioactivity. Finally, SEM micrographs of laminin-  
10 containing hydrogels showed the alignment of loaded SCs in a preferential direction forming  
11 tubular structures similar to the bands of Büngner. These findings suggested that hydrogel  
12 composition mimicking native ECM are advantageous in terms of cell organization and  
13 functionality.

14 Concerning cellular therapy, the use of hydrogel as a cell-laden construct is advantageous since they  
15 protect encapsulated cells from the immune system in the in vivo environment and ensure the  
16 homogeneous distribution of cells in the injured zone. On the other hand, to achieve an effective  
17 and prolonged cellular therapy, hydrogels should be designed to protect transplanted cells against  
18 death-mediating mechanisms (such as inflammation and oxidative stress) and to be permeable to  
19 nutrients to guarantee long term cells survival (Ritfeld et al., 2014). Permeability is an essential  
20 parameters in cell-laden hydrogel design to enable oxygen and nutrients transport and depends  
21 strongly on polymeric material chemistry as well as on network structure of the hydrogels (Nafea et  
22 al., 2014). Briefly, hydrogel mesh size is correlated with hydrogel permeability to solutes of  
23 different sizes and shapes since it provides an average measure of the space available between the  
24 macromolecular chains. This intrinsic nano-porosity can be associated to macroporosity to facilitate  
25 nutrient transfer, vascularization and cell survival (Desai et al., 2012). Traditional techniques  
26 developed for introducing macroporosity into hydrogel-based scaffolds generally result in spherical

1 macropores formation and fabrication conditions that are potentially cytotoxic (use of organic  
2 solvents, high temperature, non-physiological pH). To overcome these limitations, Hammer et al.  
3 (Hammer et al., 2014) assessed a new and cell-friendly method to fabricate 50–200  $\mu\text{m}$  size  
4 microchannels within the 3D structure of gelatin-based hydrogels. Calcium alginate (Ca-Alg)  
5 microfibers containing cells were fabricated by wet-spinning and then encapsulated within  
6 photocrosslinkable hydrogels composed of methacrylated gelatin (Gel-MA). The ability of alginate  
7 to dissolve upon exposure to ethylenediaminetetraacetic acid (EDTA) was exploited to form the  
8 microchannels inside the Gel-MA hydrogel. After EDTA treatment, cells within Ca-Alg hydrogels  
9 were released and adhered to the microchannel walls forming mono-layered cell colonies along the  
10 lumen wall of microchannels. The obtained three-dimensional microchannel-like porosity are  
11 recommended for many tissue engineering applications especially in the peripheral nervous system  
12 where nerves bundles are characterized by microfibrinous structures. Furthermore, the possibility to  
13 homogeneously distribute cells inside the microchannels prior to in vivo implantation is an important  
14 feature for the development of cellularized scaffolds able to strongly enhance the regeneration  
15 process.

16 Recently, mesenchymal stem cells (MSCs) have been proposed as transplantable cells in alternative  
17 to glial cells. MSCs have also been reported to differentiate in vitro and in vivo into non-  
18 mesodermal cell types such as neurons and astrocytes (Phinney and Isakova, 2005; Scuteri et al.,  
19 2011). The presence of MSC into porous PCL tubes have been reported to increase the number of  
20 myelinated fibers compared empty tubes in the treatment of median nerves (Oliveira et al., 2014).

21

### 22 *3.2 Rapid prototyping techniques*

23 The fabrication of novel microstructured scaffolds involves innovative techniques based on rapid  
24 prototyping (RP) that is an emerging manufacturing process used to produce complicated 3D  
25 structures automatically using computer-aided designs (CADs). Several RP techniques are now  
26 available, such as membrane lamination, ink-jet printing and fused deposition modeling, and can be



1 applied to process biocompatible and biodegradable polymers. RP techniques allow the preparation  
2 of scaffolds with complex controlled geometry, having a porosity degree up to 90%, interconnected  
3 pores and reproducible pore size and density distribution (Leong et al., 2003). RP processes have  
4 been recently adapted and utilized to form nerve conduits with precise dimensions and complex  
5 internal structures (Cui et al., 2009; Radulescu et al., 2007; Yamada et al., 2008). An ink-jet  
6 microdispensing system was developed by Radulescu et al. (Radulescu et al., 2007) for preparing a  
7 cylindrical shape scaffold that can be applied as NGCs. A PLA/PCL 80/20 copolymer was selected  
8 since it displayed good cell adhesion and proliferation of human embryonic kidney cells genetically  
9 modified to produce nerve growth factor (hNGF-EcR-293) acting as nerve growth factor release  
10 system when implanted in vivo. The presence of nerve growth factors at the injured site can  
11 strongly enhance the regeneration process (Chung et al., 2011). After selecting the appropriate  
12 polymer for cell survival, authors set up the solution parameters (concentration and solvent) to  
13 obtain an injectable solution and adjusted the ink-jet microdispenser parameters (motion speed,  
14 layer dimension, printing pattern) to fabricate the required scaffold shape. Finally, cylindrical shape  
15 conduits based on PLA/PCL 80/20 were fabricated showing the ability to maintain hNGF-EcR-293  
16 vitality.

17 FDM technique was optimized by Yamata et al. (Yamada et al., 2008) to be applied for tissue  
18 engineering scaffold fabrication. A novel method for three-dimensional microstructures fabrication  
19 was developed based on FDM technologies. Biodegradable aliphatic polyesters (PLA, PGA and  
20 PLGA) were processed avoiding the use toxic solvents and microstructures of different shapes were  
21 obtained having a resolution of 45 $\mu$ m. PC12 cells showed similar morphology and proliferation rate  
22 when cultured on microfabricated PLA substrate compared to standard plate.

23 Cui et al. (Cui et al., 2009) prepared a double layer polyurethane-collagen NGC via a double nozzle,  
24 low temperature, deposition manufacturing (DLDM) system, followed by post-processing (by  
25 thermally induced phase separation and freeze-drying). One nozzle was fed with collagen solution  
26 to obtain the inner guide layer, while the other nozzle was fed with a polyurethane solution in

1 dioxane to form the external NGC layer. Porosity degree of the external layer was increased from  
2 74% to 82% with increasing polyurethane solution concentration from 8 to 12% (w/v). The inner  
3 collagen layer showed a fibrous structure with nanosized filaments, while the outer polyurethane  
4 layer showed pores with size from 15 to 25  $\mu\text{m}$ . DLDM technique was advantageous as it allowed  
5 the obtainment of a double layered NGC with a regular and reproducible architecture in a single  
6 process. Moreover, low temperature processing is advantageous as it could allow the incorporation  
7 of growth factors and cells during scaffold fabrication.

8 In-depth biological characterization of NGCs obtained using rapid prototyping techniques is still  
9 lacking and further evaluations are required to assess their applicability in peripheral nerve  
10 regeneration.

11

#### 12 **4. Design trends**

13 Current available and FDA approved bioresorbable NGCs are not recommended for larger gaps  
14 than 3 cm (Kehoe et al., 2012) and their biological performances are inferior to autograft that  
15 remains the gold standard treatment for bridging approaches. The effective permeation of nutrients  
16 and prevention of fibrous scar tissue invasion as well as the good mechanical strength of the tube to  
17 maintain a stable support structure for the nerve regeneration are the fundamental features of  
18 artificial guides to be successfully applied as NGCs.

19 The current trend of peripheral nerve tissue engineering is to design advanced NGCs having internal  
20 structures providing topographic, chemotactic and haptotactic cues able to increase the axon  
21 regenerating rate, thus avoiding or minimizing end-organ (e.g. muscle) atrophy. In the case of large  
22 nerve gap (> 2cm), NGCs design should be inspired by biomimetic principles: NGCs should  
23 resemble the native architecture of the peripheral nerve and provide directional guidance to  
24 regenerating axons. Furthermore to improve the biological outcomes, new strategies to enhance the  
25 regeneration process based on cell-loaded fillers are under investigation.

1 Summarizing the features described above, the external guide of NGCs should satisfy the following  
2 requirements:

- 3 • Mechanical properties close to those of a human nerve: E values in 8-16 MPa range, UTS  
4 values comprised between 6.5-8.5 MPa and  $\epsilon$  of around 0.6-1.6 mm $\cdot$ mm<sup>-1</sup> The guide should  
5 be resilient in order to be sutured at the nerve ends without any decrease in its mechanical  
6 performance. In addition, the guide should be resistant to the compression stresses deriving  
7 from the formation of external fibrotic tissue; finally, it should be able to bend without  
8 kinking.
- 9 • Porosity degree higher than 50% with an optimal value of around 70%, allowing the guide  
10 to be permeable to nutrients and waste products. Porosities higher than 80% generally cause  
11 guide mechanical instability (Kokai et al., 2009; Wen and Tresco, 2006).
- 12 • Pore size of around 5-30  $\mu$ m (with optimal values of 10-20  $\mu$ m), to allow nutrient and waste  
13 products permeation and the infiltration of blood vessels and to protect the regeneration  
14 environment from the infiltration of scar tissue, although avoiding the outflow of the growth  
15 factors secreted by the distal nerve stump.
- 16 • Guide wall thickness selected on the basis of the mechanical requirements, target  
17 degradation rate, permeability specifications and easy suturability. Guide thickness up to  
18 200  $\mu$ m allows nutrient diffusion, while a value of 600  $\mu$ m is the maximum guide thickness  
19 value as it is associated with minimal diffusion (Kokai et al., 2009). Guides have been  
20 generally prepared with a thickness of around 100-300  $\mu$ m.
- 21 • Diameter of the conduit tailored to the nerve size, avoiding nerve compression caused by  
22 degradation-induced swelling. A lower NGC diameter than nerve size may cause chronic  
23 nerve compression resulting in nerve damage (Mackinnon et al., 1984). On the other hand, a  
24 larger NGC diameter than nerve size may fail to support the regenerating nerve.
- 25 • Suitable NGC length, to facilitate the bridging of the nerve gap, without tension.
- 26 • Tailored degradation rate respect to the nerve tissue regeneration rate.

- 1 • Limited swelling degree during degradation to avoid reduction in the conduct lumen.

2 The NGC internal filler should satisfy the following requirements:

- 3 • It should provide *haptotactic cues* for SCs adhesion and migration. For this reason, the use  
4 of natural polymers naturally constituting ECM (e.g. collagen) or with similar composition  
5 to ECM components (e.g. gelatin, chitosan), as well as bioactive peptides (e.g. IKVAV,  
6 YIGSR), is recommended for filler materials, as they can specifically interact with SCs via  
7 integrin receptors.

- 8 • It should be porous with porosity degree of around 60-80% and pore size of 30-50  $\mu\text{m}$  to  
9 allow SCs migration from the proximal to the distal end.

- 10 • It should be degradable with a rate depending on axon regeneration rate not to obstacle  
11 axon growth.

- 12 • Swelling degree should be limited to avoid compression of regenerating axons.

- 13 • It should additionally provide directional guidance (*topographical cues*) to further enhance  
14 regeneration rate. To this purpose, the introduction of fillers based on aligned fibers or  
15 provided with longitudinally oriented channels could be advantageous.

16 NGC presenting the above listed features have been shown to achieve nerve regeneration at the  
17 injured site with regenerated nerves characterized by cables having a smaller area, fibre diameter  
18 and density compared to normal nerves. The encouraging results obtained in the last decade with  
19 NGCs still show inferior performances than autograft. To overcome these limitations, advanced  
20 NGCs than can revolutionize the biological performances of artificial grafts should introduce  
21 growth factors or cells into the conduit lumen. Innovative NGCs should be designed:

- 22 • to provide *chemotactic cues* by the incorporation and release of growth factors.
- 23 • To introduce cells into the guide lumen, mainly exploiting the paracrine effect of the  
24 implanted cells towards nerve regeneration. Typically, autologous SCs or mesenchymal and  
25 neural stem cells have been tested (Gu et al., 2011). Implanted cells keep viable for some  
26 weeks, depositing their ECM and secreting growth factors which can stimulate regeneration.

1 However, their integration or differentiation into glial cells have never been demonstrated.  
 2 In addition, the use of cellularised fillers (Galla et al., 2004; Suri and Schmidt, 2010;  
 3 Thompson and Buettner, 2001) make method industrialization and translation into clinics  
 4 difficult, with high cost of the final product.

5 Previous reviews have been focused on materials used for NGCs, including the functionalisation  
 6 with peptides, growth factors or the use of cells within the tube lumen (Gu et al., 2011). The aim of  
 7 this work was that to provide an overview on architectural design of NGCs, which is currently  
 8 lacking in the scientific literature. The manufacturing techniques for the preparation of NGCs are  
 9 listed in **Table 3** together with commonly attainable architectural features (porosity degree and pore  
 10 size).

11  
 12 **Table 3. General features of the manufacturing techniques employed to fabricate NGCs: main**  
 13 **process parameters and average porosity degree and pore size of the final NGC substrate.**

Technique	Main process parameters	Porosity degree (%)	Pore size ( $\mu\text{m}$ )	Ref
Electrospinning	<ul style="list-style-type: none"> <li>• Solution concentration</li> <li>• Electric field</li> <li>• Collector type</li> <li>• Syringe tip-collector distance</li> <li>• Flow rate</li> </ul>	58-95	1-10 $\mu\text{m}$	(Chew et al., 2007; Wang et al., 2008)
Porogen leaching	<ul style="list-style-type: none"> <li>• Porogen (salt or polymer) amount</li> <li>• Size of porogen salt crystals</li> <li>• Compatibility of polymer blends</li> </ul>	80-90	<ul style="list-style-type: none"> <li>• 0.9-5 <math>\mu\text{m}</math> (poly(ethylene glycole), PEG)</li> <li>• 10-300 <math>\mu\text{m}</math> (NaCl)</li> </ul>	(Kokai et al., 2009; Matsumoto et al., 2000; Tonda-Turo et al., 2011a; Widmer et al., 1998; Yucel et al., 2010)
Freeze-Drying	<ul style="list-style-type: none"> <li>• Solution concentration</li> <li>• Freezing temperature</li> <li>• Temperature gradient during freezing</li> </ul>	~ 90	10-300 $\mu\text{m}$	(Bozkurt et al., 2012; Tonda-Turo et al., 2011a; Wang et al., 2012)
Thermally induced phase separation (TIPS)	<ul style="list-style-type: none"> <li>• Solution concentration</li> <li>• Temperature of phase separation</li> <li>• Temperature gradient during cooling</li> </ul>	85-90	15-140 $\mu\text{m}$	(Ao et al., 2006; Sun et al., 2012)

Non solvent induced phase separation (NIPS)	<ul style="list-style-type: none"> <li>• Solution concentration</li> <li>• Solvent/Non-solvent pair</li> </ul>	-	50 nm -50 $\mu$ m	(Chiono et al., 2008b; Hsu and Ni, 2009; Oh et al., 2008)
Rapid Prototyping (RP)	<ul style="list-style-type: none"> <li>• Unit cell geometry and size</li> <li>• Layer assembly method</li> <li>• Layer number and their reciprocal orientation</li> </ul>	Controlled and reproducible: 75-90, generally	As required	(Cui et al., 2009; Radulescu et al., 2007; Yamada et al., 2008)

1

2 On the basis of **Table 3** data and previous discussion, electrospinning, porogen leaching and NIPS  
3 are suitable manufacturing techniques for the fabrication of external guides having suitable  
4 mechanical properties and permeability, whereas inner fillers may be prepared by freeze-drying,  
5 electrospinning or TIPS where aligned and oriented porous structures showed improved results  
6 compared to randomly oriented pores due to their biomimetic morphology. In addition, injectable  
7 hydrogels are also advantageous as NGC fillers for both growth factors release and cell  
8 encapsulation (cellular therapy).

9 Complex NGCs consisting of an external guide and a filler may be assembled by different  
10 procedures. For instance, aligned electrospun fibers may be placed on the surface of porous  
11 membranes, which are then rolled and longitudinally glued (Okamoto et al., 2010; Yucel et al.,  
12 2010). This technique allows the preparation of composite conduit during surgery, adapting NGC  
13 diameter to that of the regenerating nerve. Alternatively porous guides may be prepared and then  
14 filled with freeze-dried porous matrices or injectable hydrogels (Gu et al., 2011).

15 Composite conduits entirely based on natural polymers, such as collagen, have been shown to have  
16 higher degradation rate than that required for the regeneration of severe (> 30 mm) nerve defects  
17 (Okamoto et al., 2010). Ideally, the external guide should be based on a slowly degrading and  
18 mechanically resistant material, such as a biocompatible synthetic polymer. On the other hand, the  
19 inner matrix should be based on natural polymers, providing haptotactic cues for the adhesion and  
20 migration of SCs.

1 Finally, RP methods are emerging techniques for NGC manufacturing, allowing computer-driven  
2 design of scaffolds with desired architecture. RP allows the obtainment of structures with  
3 reproducible geometry, for easy industrialization. However, the relatively high cost of this  
4 manufacturing technique currently limits its diffusion.

5 A wide range of in vitro and in vivo experimental settings to test developed NGCs have been  
6 reported making difficult a direct comparison of the different results. Therefore, the adoption of  
7 standardized experimental conditions and assays should be encouraged for a correct interpretation  
8 of the biological response to the implantation of different NGCs.

9

## 10 **5. Conclusions**

11 The combination of different cues in a single device is expected to maximize the influence of the  
12 guidance signaling and could be promising for the repair of large nerve gaps. The external guide  
13 should satisfy different requirements: it should display biomimetic mechanical properties, 50-80%  
14 porosity degree with ideal pore size of 5-30  $\mu\text{m}$  and tailored degradation rate. Biocompatible  
15 synthetic polymers are the ideal candidate materials to be used for the preparation of external  
16 tubular conduits for NGCs, due to their high mechanical properties and shape stability in  
17 physiological media, while NIPS, particulate leaching and electrospinning are the preferred  
18 methods to satisfy architectural requirements of tubular guides. For instance, the authors proposed  
19 the preparation of PCL guides by PEO leaching technique, having pores with 0.9  $\mu\text{m}$  size,  
20 biomimetic mechanical properties and suitable permeability (Tonda-Turo et al., 2011a).  
21 Alternatively, the authors proposed the use of highly crosslinked natural polymers as external  
22 tubular conduits which can be easily rolled into tubes with desired size.

23 Inner filler for NGCs should satisfy the following main requirements: porosity degree of 60-80 %,  
24 pore size of around 30-50  $\mu\text{m}$ , suitable degradation rate respect to axon regeneration rate and  
25 limited swelling to avoid axon compression. Natural polymer inner fillers for NGCs can be  
26 prepared in the form of fibers, gels and sponges; providing haptotactic and topographical cues to

1 regenerating axons. Aligned electrospun mats may be easily inserted into guides prepared from  
2 rolled membranes; on the other hand, gels may be injected into tubular conduits, while sponges may  
3 be prepared by freeze-drying or TIPS within the tubular conduits. The authors proposed different  
4 types of gelatin based fillers: electrospun gelatin nanofibers (Tonda-Turo et al., 2013), freeze-dried  
5 gelatin sponges (Tonda-Turo et al., 2011a) and injectable agar/gelatin gels (Tonda-Turo et al.,  
6 2014). Finally, RP methods represent advanced approaches for the preparation of complex guides  
7 with highly reproducible and controlled morphology, provided with inner coating or filler, by a  
8 single step procedure.

9 Biomimetic internal structures having directional cues showed improved performance in terms of  
10 regeneration even if the autologous graft remains the gold standard approach. To achieve a step  
11 forward in the field and encourage the use of artificial grafts in the clinics, multifunctional devices  
12 combining topographical, haptotactic and chemotactic cues should be investigated in-depth.  
13 Furthermore, cellularized matrices, exploiting both the paracrine and the exogenous effects, have  
14 shown preliminary promising results and have opened new possibilities in the treatment of large gap  
15 nerve injuries.

16

## 17 **Acknowledgements**

18 This work was supported by the Regione Piemonte (BICONERVE project). A special thank to  
19 Clara Mattu for SEM micrographs.

20

21

22

23

24

25

26



1 **Figure Captions**

2

3 **Figure 1.** Schematic representation of the structural features of nerve guidance channels, designed  
4 to regenerate peripheral nerves. Depicted strategies include the use of porous and not porous single  
5 lumen NGCs surface functionalised with biomimetic molecules or having micro-grooved luminal  
6 designs; intraluminal guidance structures such as fibers, sponges and gels; multi-channel NGCs to  
7 provide topographical guidance to regenerating axons and migrating Schwann cells and  
8 combinatorial approaches. Reproduced with permission from (Daly et al., 2012).

9 **Figure 2.** SEM micrographs of A) electrospun membrane rolled and sealed into tubes (reproduced  
10 with permission from (Chew et al., 2007)); B) electrospun PLGA/PCL nerve guide conduit  
11 (reproduced with permission from (Panseri et al., 2008)); C) bundle composed of aligned fibres  
12 (reproduced with permission from (Teo and Ramakrishna, 2005)).

13 **Figure 3.** SEM micrograph of A, B) PCL porous guide by Kokai et al., 2009 (reproduced with  
14 permission from (Kokai et al., 2009)); C,D) PCL porous guide by Tonda-Turo et. al, 2011a  
15 (reproduced with permission from (Tonda-Turo et al., 2011a)) ; E,F) PU60i tube (bar: A, C, E 500  
16  $\mu\text{m}$ ; B, D,F 100  $\mu\text{m}$ )

17 **Figure 4.** Percentage of FD-4 concentration in the external releasing medium respect to the initial  
18 FD-4 concentration filling the tube as a function of time, for not porous and porous PCL conduits.  
19 Data are average values  $\pm$  standard deviation (n=3).

20

21 **Figure 5.** A) SEM micrograph of a fractured section of the PCL60i tube filled with GL/GP sponge.  
22 (reproduced with permission from (Tonda-Turo et al., 2011a)). B) SEM micrograph of heparan  
23 sulfate proteoglycan (HSPG)/collagen scaffolds (reproduced with permission from(Wang et al.,  
24 2012)). C,D) Perimaix nerve guides. C: SEM of the longitudinal microstructure of the Perimaix  
25 nerve guide; D: SEM of the transverse microstructure (reproduced with permission from (Bozkurt  
26 et al., 2012)).Scale bars: A 500  $\mu\text{m}$ , B 100  $\mu\text{m}$ , C-D 200  $\mu\text{m}$ .

27 **Figure 6.** Scanning electron microscopy (SEM) micrographs of: A) CS/GPTMS membranes frozen  
28 at  $-20^{\circ}\text{C}$  (bar: 200  $\mu\text{m}$ ) and B) of the fractured section of CS/GPTMS tube obtained by wrapping  
29 flat membrane (bar: 500  $\mu\text{m}$ ). The arrow indicates the zone where the membrane was glued to  
30 obtain the circular shape. The insert is an image of a CS/GPTMS membrane as demonstration of its  
31 flexibility.

32 **Figure 7.** SEM micrographs of A) cross-sectional, inner, and outer surfaces of PLGA/F127 (3  
33 wt%) (reproduced with permission from (Oh et al., 2008)); B) PHBHV/PCL 50/50 (wt./wt.)  
34 (reproduced with permission from (Chiono et al., 2008b)). Scale bars:B-C 10  $\mu\text{m}$ .

35 **Figure 8.** SEM micrographs of 4-channel nanofibrous PLLA scaffold (reproduced with permission  
36 from (Sun et al., 2012).

37 **Figure 9.** Porous CS hollow guide filled with A/GL\_GP injectable hydrogels: A) image of  
38 A/GL\_GP hydrogel injected into the hollow CS guide, B) SEM micrograph of freeze-dried  
39 A/GL\_GP hydrogel (scale bar 100  $\mu\text{m}$ ).

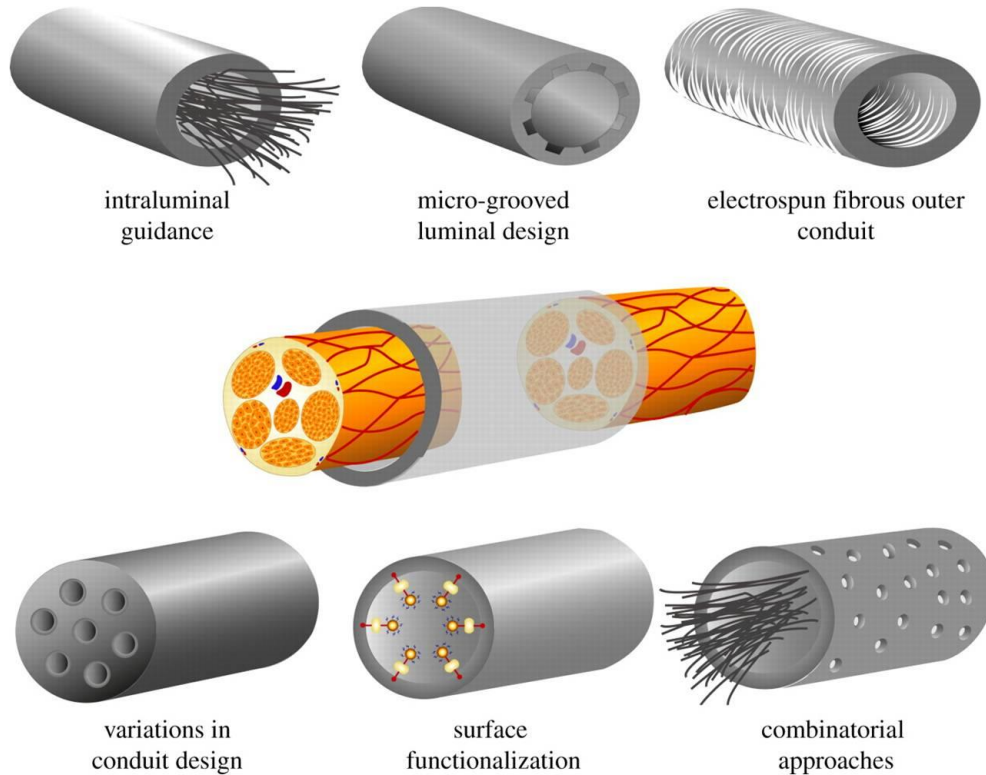
40

1 **Figure 10.** Classification of techniques used for external guide and internal filler fabrication.  
 2 Schematic representation of NGC typologies: A) hollow tube; B) flat membranes rolled and  
 3 longitudinally sutured or glued into hollow guides; C) internal fillers as injectable hydrogel, porous  
 4 or oriented matrices filling the guide luminal cavity; and D) bi- or multi-layered guides having one  
 5 or more internal fillers covering the internal surface of the guide.

6

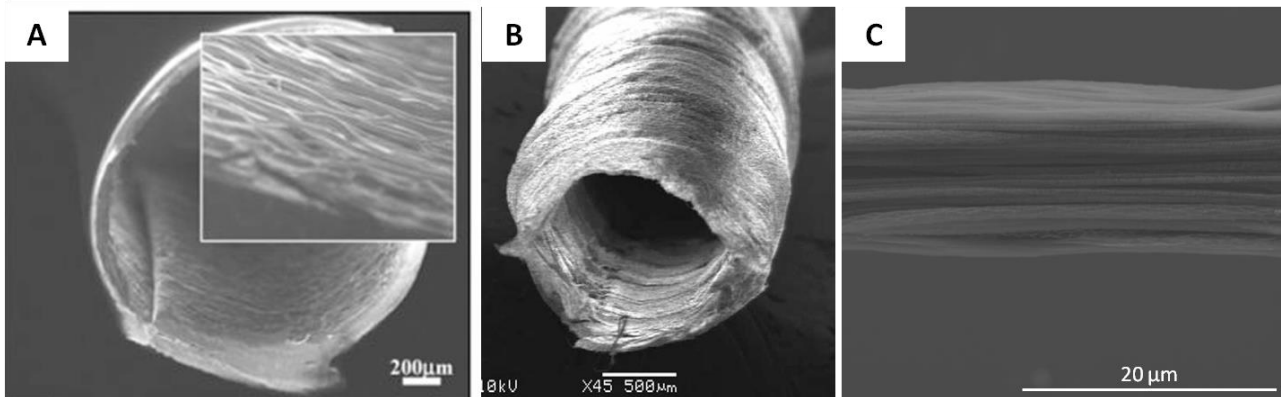
7

8 **FIGURES**



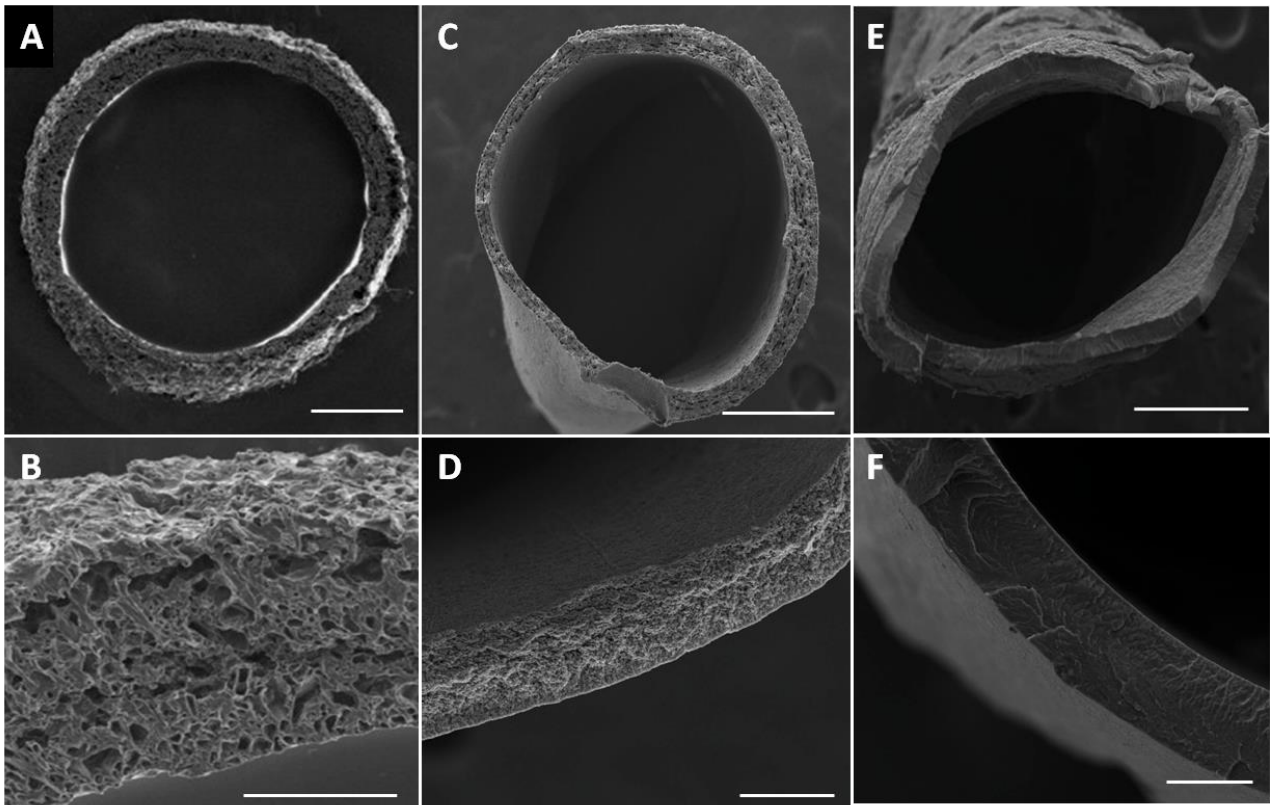
9  
10  
11 **Figure 1**

12



13  
14  
15 **Figure 2**

16  
17



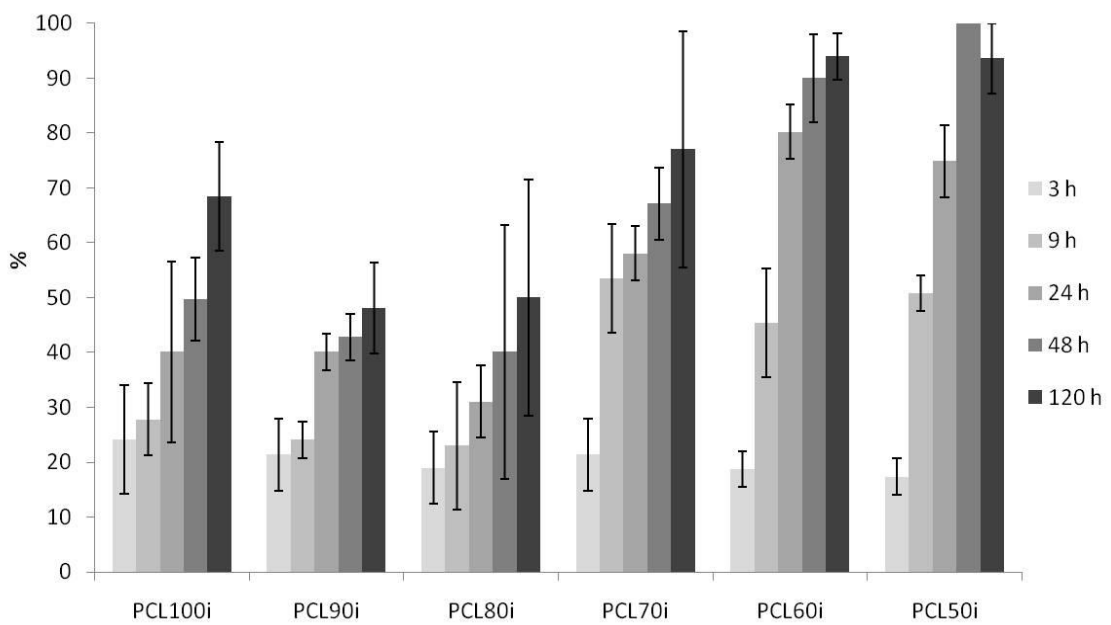
1

2

3

4

**Figure 3**

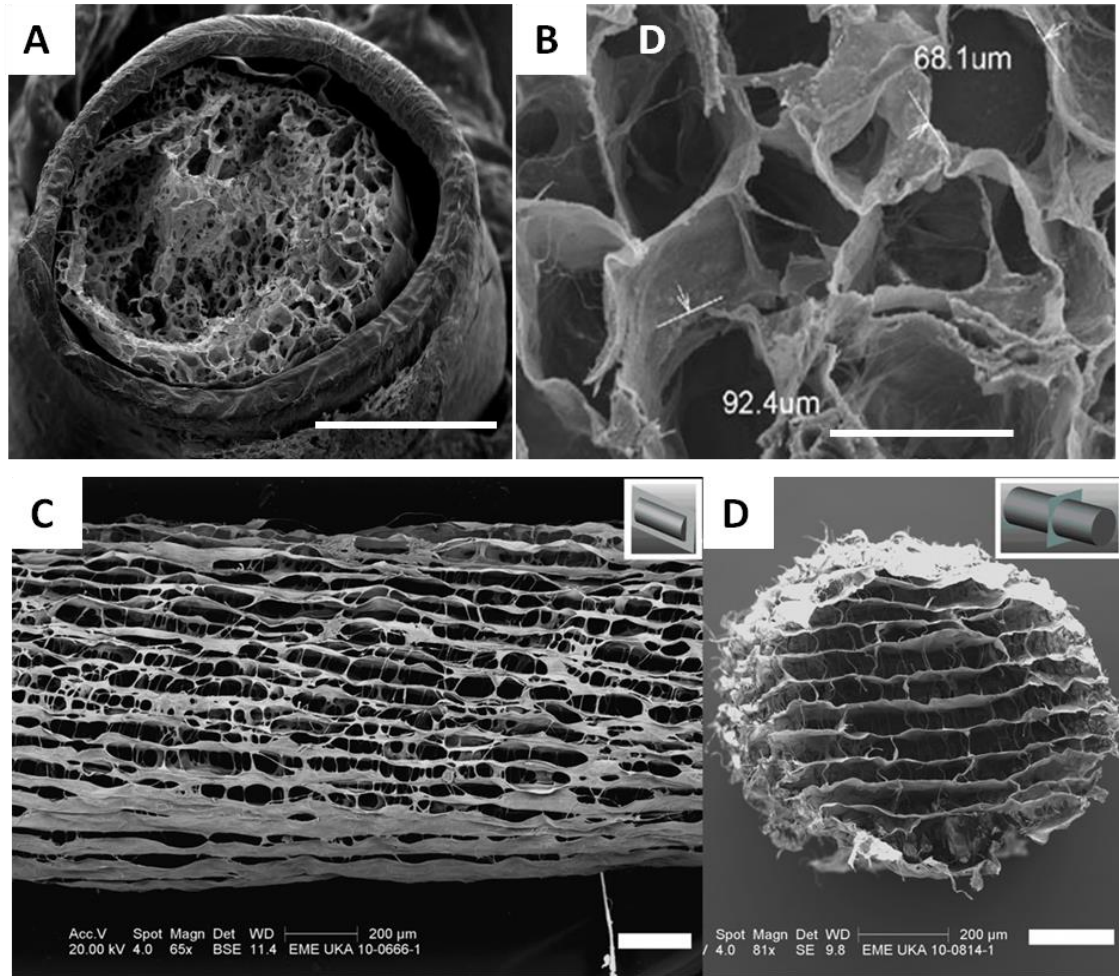


5

6

**Figure 4**

1

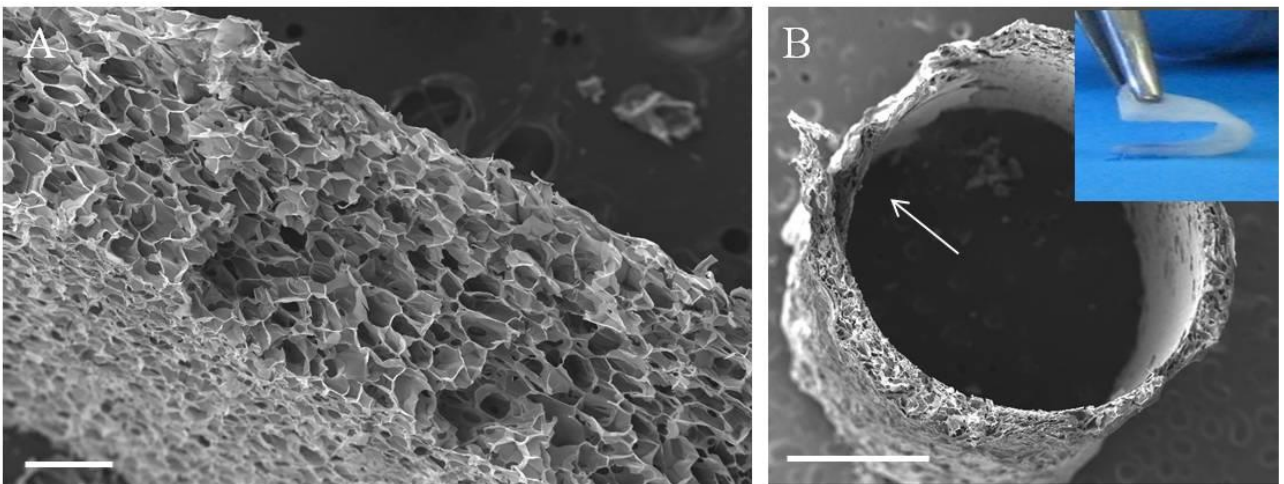


2

3

4

Figure 5

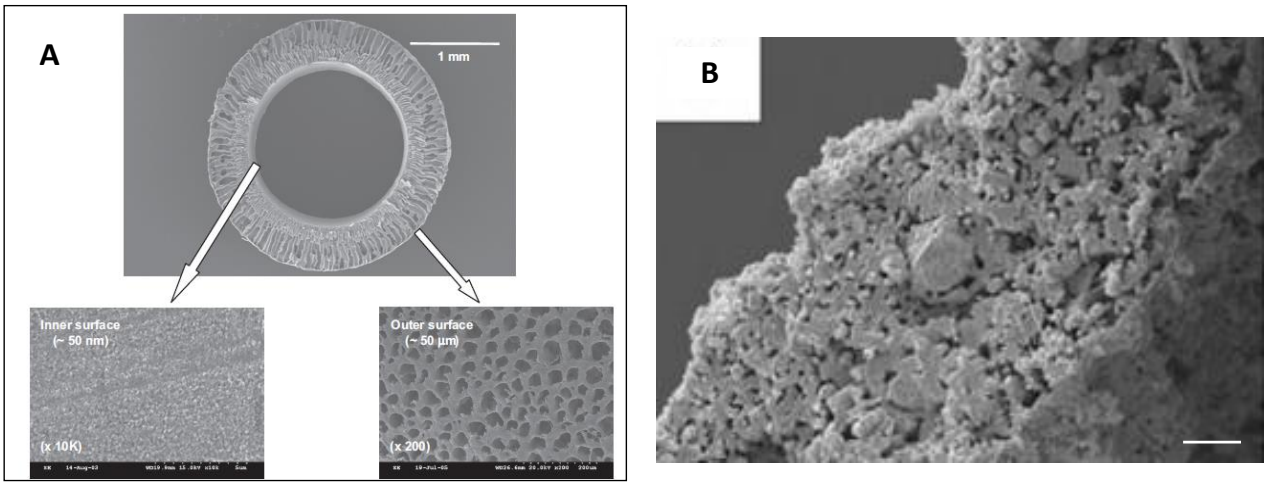


5

6

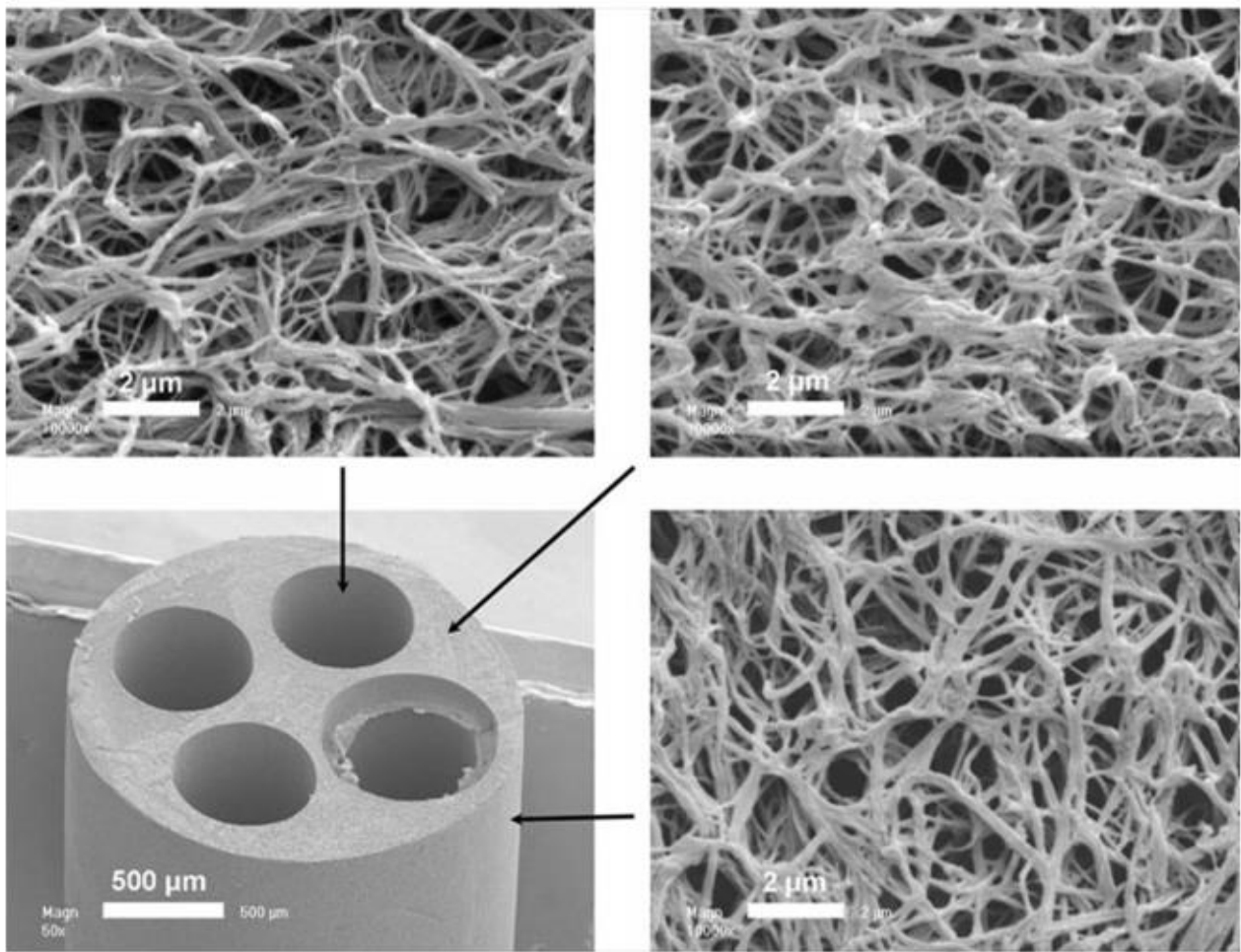
7

Figure 6



1  
2  
3

**Figure 7**



4  
5  
6  
7

**Figure 8**

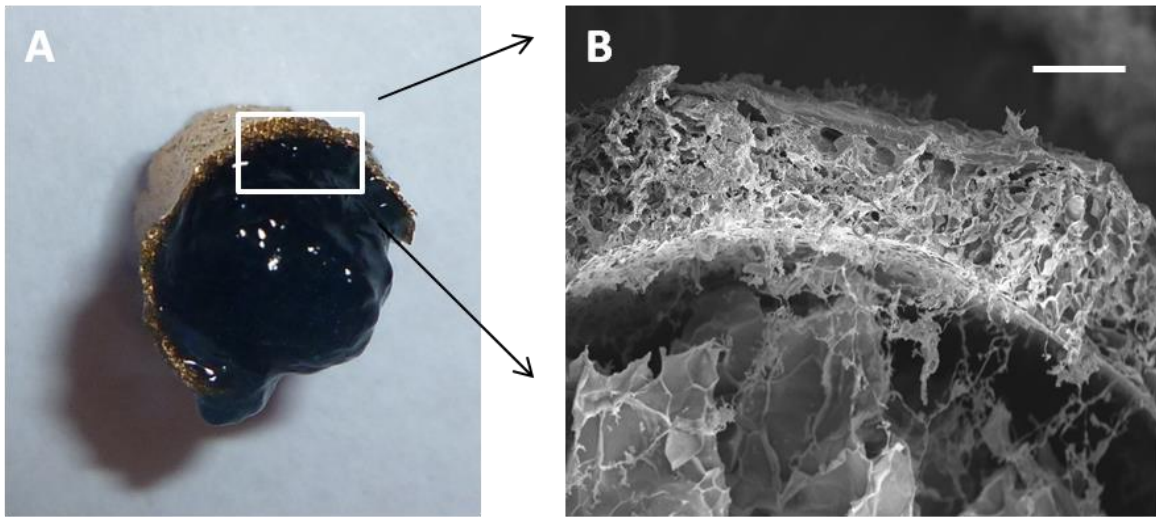


Figure 9

1  
2  
3

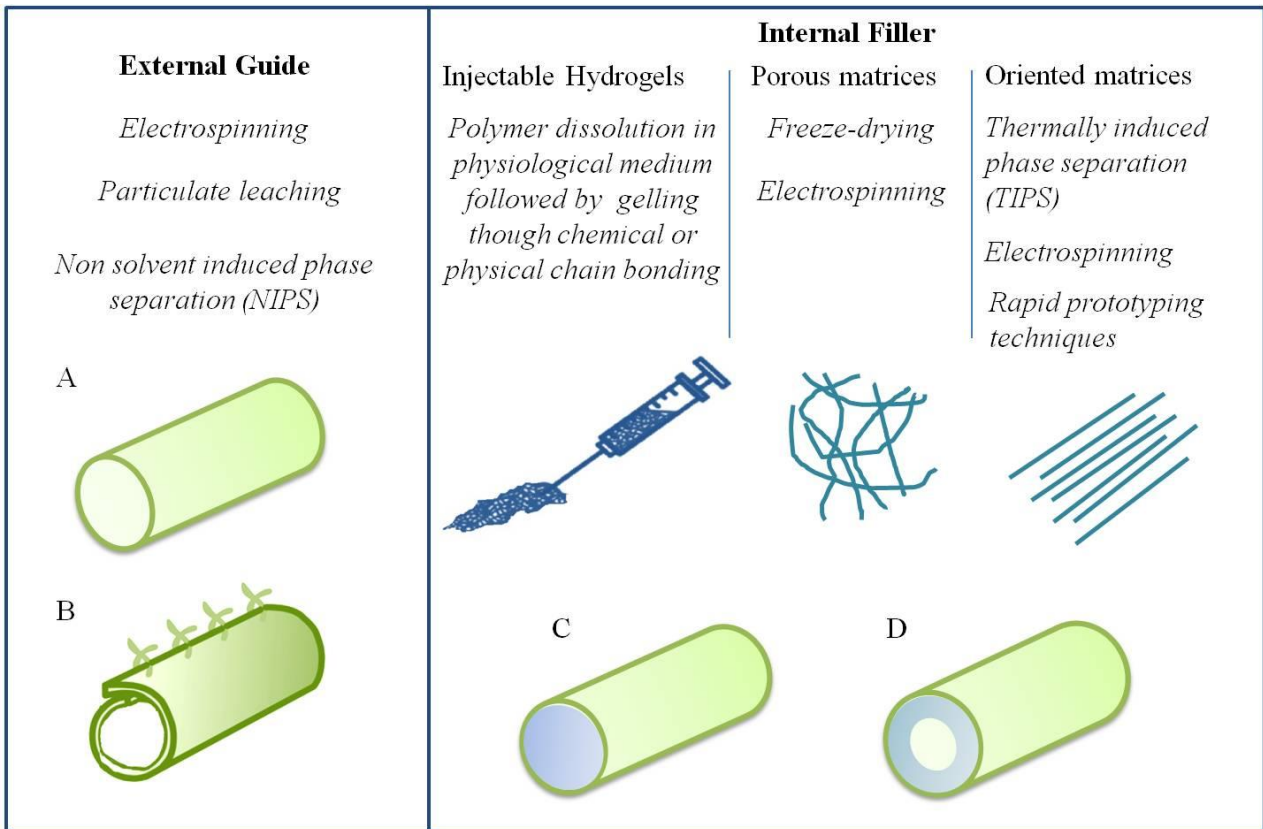


Figure 10

4  
5  
6  
7  
8  
9

## 1 References

- 2 A.B. Sanghvi, J.L.M., C.E. Schmidt. 2004. Encyclopedia of biomaterials and biomedical engineering. Marcel  
3 Dekker Inc., New York. 1613 pp.
- 4 Ao, Q., A.J. Wang, W.L. Cao, L. Zhang, L.J. Kong, Q. He, Y.D. Gong, and X.F. Zhang. 2006. Manufacture of  
5 multimicrotubule chitosan nerve conduits with novel molds and characterization in vitro. *Journal*  
6 *of Biomedical Materials Research Part A*. 77A:11-18.
- 7 Balgude, A.P., X. Yu, A. Szymanski, and R.V. Bellamkonda. 2001. Agarose gel stiffness determines rate of  
8 DRG neurite extension in 3D cultures. *Biomaterials*. 22:1077-1084.
- 9 Battiston, B., S. Raimondo, P. Tos, V. Gaidano, C. Audisio, A. Scevola, I. Perroteau, and S. Geuna. 2009.  
10 Chapter 11: Tissue engineering of peripheral nerves. *Int Rev Neurobiol*. 87:227-249.
- 11 Bian, Y.Z., Y. Wang, G. Aibaidoula, G.Q. Chen, and Q. Wu. 2009. Evaluation of poly(3-hydroxybutyrate-co-  
12 3-hydroxyhexanoate) conduits for peripheral nerve regeneration. *Biomaterials*. 30:217-225.
- 13 Bini, T.B., S.J. Gao, T.C. Tan, S. Wang, A. Lim, L.B. Hai, and S. Ramakrishna. 2004. Electrospun poly(L-  
14 lactide-co-glycolide) biodegradable polymer nanofibre tubes for peripheral nerve regeneration.  
15 *Nanotechnology*. 15:1459-1464.
- 16 Borschel, G.H., K.F. Kia, W.M. Kuzon, Jr., and R.G. Dennis. 2003. Mechanical properties of acellular  
17 peripheral nerve. *J Surg Res*. 114:133-139.
- 18 Boyle, M.D., A.P. Gee, and T. Borsos. 1979. Studies on the terminal stages of immune hemolysis. VI.  
19 Osmotic blockers of differing Stokes' radii detect complement-induced transmembrane channels  
20 of differing size. *J Immunol*. 123:77-82.
- 21 Bozkurt, A., F. Lassner, D. O'Dey, R. Deumens, A. Bocker, T. Schwendt, C. Janzen, C.V. Suschek, R. Tolba,  
22 E. Kobayashi, B. Sellhaus, S. Tholl, L. Eummelen, F. Schugner, L.O. Damink, J. Weis, G.A. Brook,  
23 and N. Pallua. 2012. The role of microstructured and interconnected pore channels in a collagen-  
24 based nerve guide on axonal regeneration in peripheral nerves. *Biomaterials*. 33:1363-1375.
- 25 Brunelli, G.A., B. Battiston, A. Vigasio, G. Brunelli, and D. Marocolo. 1993. Bridging nerve defects with  
26 combined skeletal muscle and vein conduits. *Microsurgery*. 14:247-251.
- 27 Ceballos, D., X. Navarro, N. Dubey, G. Wendelschafer-Crabb, W.R. Kennedy, and R.T. Tranquillo. 1999.  
28 Magnetically aligned collagen gel filling a collagen nerve guide improves peripheral nerve  
29 regeneration. *Exp Neurol*. 158:290-300.
- 30 Chen, M.B., F. Zhang, and W.C. Lineaweaver. 2006. Luminal fillers in nerve conduits for peripheral nerve  
31 repair. *Ann Plast Surg*. 57:462-471.
- 32 Chew, S.Y., R. Mi, A. Hoke, and K.W. Leong. 2007. Aligned Protein-Polymer Composite Fibers Enhance  
33 Nerve Regeneration: A Potential Tissue-Engineering Platform. *Adv Funct Mater*. 17:1288-1296.
- 34 Chiono, V., G. Ciardelli, G. Vozzi, J. Cortez, N. Barbani, P. Gentile, and P. Giusti. 2008a. Enzymatically-  
35 modified melt-extruded guides for peripheral nerve repair. *Eng Life Sci*. 8:226-237.
- 36 Chiono, V., G. Ciardelli, G. Vozzi, M.G. Sotgiu, B. Vinci, C. Domenici, and P. Giusti. 2008b. Poly(3-  
37 hydroxybutyrate-co-3-hydroxyvalerate)/poly(epsilon-caprolactone) blends for tissue engineering  
38 applications in the form of hollow fibers. *Journal of Biomedical Materials Research Part A*.  
39 85A:938-953.
- 40 Chiono, V., S. Sartori, A. Rechichi, C. Tonda-Turo, G. Vozzi, F. Vozzi, M. D'Acunto, C. Salvadori, F. Dini, G.  
41 Barsotti, F. Carlucci, S. Burchielli, S. Nicolino, C. Audisio, I. Perroteau, P. Giusti, and G. Ciardelli.  
42 2011. Poly(ester urethane) guides for peripheral nerve regeneration. *Macromol Biosci*. 11:245-  
43 256.
- 44 Chiono, V., C. Tonda-Turo, and G. Ciardelli. 2009a. Chapter 9: Artificial scaffolds for peripheral nerve  
45 reconstruction. *Int Rev Neurobiol*. 87:173-198.
- 46 Chiono, V., G. Vozzi, F. Vozzi, C. Salvadori, F. Dini, F. Carlucci, M. Arispici, S. Burchielli, F. Di Scipio, S.  
47 Geuna, M. Fornaro, P. Tos, S. Nicolino, C. Audisio, I. Perroteau, A. Chiaravalloti, C. Domenici, P.  
48 Giusti, and G. Ciardelli. 2009b. Melt-extruded guides for peripheral nerve regeneration. Part I:  
49 Poly(epsilon-caprolactone). *Biomed Microdevices*. 11:1037-1050.
- 50 Chung, T.W., M.C. Yang, C.C. Tseng, S.H. Sheu, S.S. Wang, Y.Y. Huang, and S.D. Chen. 2011. Promoting  
51 regeneration of peripheral nerves in-vivo using new PCL-NGF/Tirofiban nerve conduits.  
52 *Biomaterials*. 32:734-743.

1 Ciardelli, G., and V. Chiono. 2006. Materials for peripheral nerve regeneration. *Macromol Biosci.* 6:13-26.  
2 Cordeiro, P.G., B.R. Seckel, S.A. Lipton, P.A. Damore, J. Wagner, and R. Madison. 1989. Acidic Fibroblast  
3 Growth-Factor Enhances Peripheral-Nerve Regeneration In Vivo. *Plast Reconstr Surg.* 83:1013-  
4 1019.  
5 Crompton, K.E., J.D. Goud, R.V. Bellamkonda, T.R. Gengenbach, D.I. Finkelstein, M.K. Horne, and J.S.  
6 Forsythe. 2007. Polylysine-functionalised thermoresponsive chitosan hydrogel for neural tissue  
7 engineering. *Biomaterials.* 28:441-449.  
8 Cui, T.K., Y.N. Yan, R.J. Zhang, L. Liu, W. Xu, and X.H. Wang. 2009. Rapid Prototyping of a Double-Layer  
9 Polyurethane-Collagen Conduit for Peripheral Nerve Regeneration. *Tissue Eng Part C-Me.* 15:1-9.  
10 Daly, W., L. Yao, D. Zeugolis, A. Windebank, and A. Pandit. 2012. A biomaterials approach to peripheral  
11 nerve regeneration: bridging the peripheral nerve gap and enhancing functional recovery. *J R Soc*  
12 *Interface.* 9:202-221.  
13 de Ruitter, G.C., M.J. Malessy, M.J. Yaszemski, A.J. Windebank, and R.J. Spinner. 2009. Designing ideal  
14 conduits for peripheral nerve repair. *Neurosurg Focus.* 26:E5.  
15 de Ruitter, G.C., R.J. Spinner, M.J. Malessy, M.J. Moore, E.J. Sorenson, B.L. Currier, M.J. Yaszemski, and  
16 A.J. Windebank. 2008. Accuracy of motor axon regeneration across autograft, single-lumen, and  
17 multichannel poly(lactic-co-glycolic acid) nerve tubes. *Neurosurgery.* 63:144-153; discussion 153-  
18 145.  
19 Dellon, A.L., and S.E. Mackinnon. 1988. Basic scientific and clinical applications of peripheral nerve  
20 regeneration. *Surg Annu.* 20:59-100.  
21 Desai, E.S., M.Y. Tang, A.E. Ross, and R.A. Gemeinhart. 2012. Critical factors affecting cell encapsulation  
22 in superporous hydrogels. *Biomed Mater.* 7.  
23 Deumens, R., A. Bozkurt, M.F. Meek, M.A. Marcus, E.A. Joosten, J. Weis, and G.A. Brook. 2010. Repairing  
24 injured peripheral nerves: Bridging the gap. *Prog Neurobiol.* 92:245-276.  
25 Dodla, M.C., and R.V. Bellamkonda. 2008. Differences between the effect of anisotropic and isotropic  
26 laminin and nerve growth factor presenting scaffolds on nerve regeneration across long  
27 peripheral nerve gaps. *Biomaterials.* 29:33-46.  
28 Dumont, C.E., and W. Born. 2005. Stimulation of neurite outgrowth in a human nerve scaffold designed  
29 for peripheral nerve reconstruction. *J Biomed Mater Res B Appl Biomater.* 73:194-202.  
30 Galla, T.J., S.V. Vedecnik, J. Halbgewachs, S. Steinmann, C. Friedrich, and G.B. Stark. 2004.  
31 Fibrin/Schwann cell matrix in poly-epsilon-caprolactone conduits enhances guided nerve  
32 regeneration. *Int J Artif Organs.* 27:127-136.  
33 Georgiou, M., J.P. Golding, A.J. Loughlin, P.J. Kingham, and J.B. Phillips. 2015. Engineered neural tissue  
34 with aligned, differentiated adipose-derived stem cells promotes peripheral nerve regeneration  
35 across a critical sized defect in rat sciatic nerve. *Biomaterials.* 37:242-251.  
36 Gnani, S., L. di Blasio, C. Tonda-Turo, A. Mancardi, L. Primo, G. Ciardelli, G. Gambarotta, S. Geuna, and I.  
37 Perroteau. 2014. Gelatin-based hydrogel for vascular endothelial growth factor release in  
38 peripheral nerve tissue engineering. *J Tissue Eng Regen Med.*  
39 Gopferich, A. 1996. Mechanisms of polymer degradation and erosion. *Biomaterials.* 17:103-114.  
40 Gu, X., F. Ding, Y. Yang, and J. Liu. 2011. Construction of tissue engineered nerve grafts and their  
41 application in peripheral nerve regeneration. *Prog Neurobiol.* 93:204-230.  
42 Hammer, J., L.H. Han, X.M. Tong, and F. Yang. 2014. A Facile Method to Fabricate Hydrogels with  
43 Microchannel-Like Porosity for Tissue Engineering. *Tissue Eng Part C-Me.* 20:169-176.  
44 He, L., Y. Zhang, C. Zeng, M. Ngiam, S. Liao, D. Quan, Y. Zeng, J. Lu, and S. Ramakrishna. 2009.  
45 Manufacture of PLGA multiple-channel conduits with precise hierarchical pore architectures and  
46 in vitro/vivo evaluation for spinal cord injury. *Tissue Eng Part C Methods.* 15:243-255.  
47 Homayoni, H., S.A.H. Ravandi, and M. Valizadeh. 2009. Electrospinning of chitosan nanofibers: Processing  
48 optimization. *Carbohyd Polym.* 77:656-661.  
49 Hsu, S.H., and H.C. Ni. 2009. Fabrication of the Microgrooved/Microporous Polylactide Substrates as  
50 Peripheral Nerve Conduits and In Vivo Evaluation. *Tissue Eng Pt A.* 15:1381-1390.  
51 Huang, Y.C., and Y.Y. Huang. 2006. Biomaterials and strategies for nerve regeneration. *Artif Organs.*  
52 30:514-522.



- 1 Huang, Z.M., Y.Z. Zhang, S. Ramakrishna, and C.T. Lim. 2004. Electrospinning and mechanical  
2 characterization of gelatin nanofibers. *Polymer*. 45:5361-5368.
- 3 Ichihara, S., Y. Inada, A. Nakada, K. Endo, T. Azuma, R. Nakai, S. Tsutsumi, H. Kurosawa, and T. Nakamura.  
4 2009. Development of new nerve guide tube for repair of long nerve defects. *Tissue Eng Part C*  
5 *Methods*. 15:387-402.
- 6 Ichihara, S., Y. Inada, and T. Nakamura. 2008. Artificial nerve tubes and their application for repair of  
7 peripheral nerve injury: an update of current concepts. *Injury*. 39 Suppl 4:29-39.
- 8 Jenq, C.B., and R.E. Coggeshall. 1985. Nerve regeneration through holey silicone tubes. *Brain Res*.  
9 361:233-241.
- 10 Jha, B.S., R.J. Colello, J.R. Bowman, S.A. Sell, K.D. Lee, J.W. Bigbee, G.L. Bowlin, W.N. Chow, B.E. Mathern,  
11 and D.G. Simpson. 2011. Two pole air gap electrospinning: Fabrication of highly aligned, three-  
12 dimensional scaffolds for nerve reconstruction. *Acta Biomater*. 7:203-215.
- 13 Jiang, X., H.Q. Cao, L.Y. Shi, S.Y. Ng, L.W. Stanton, and S.Y. Chew. 2012. Nanofiber topography and  
14 sustained biochemical signaling enhance human mesenchymal stem cell neural commitment.  
15 *Acta Biomater*. 8:1290-1302.
- 16 Jiang, X., S.H. Lim, H.Q. Mao, and S.Y. Chew. 2010. Current applications and future perspectives of  
17 artificial nerve conduits. *Exp Neurol*. 223:86-101.
- 18 Jin, J., S. Limburg, S.K. Joshi, R. Landman, M. Park, Q. Zhang, H.T. Kim, and A.C. Kuo. 2013. Peripheral  
19 nerve repair in rats using composite hydrogel-filled aligned nanofiber conduits with incorporated  
20 nerve growth factor. *Tissue Eng Part A*. 19:2138-2146.
- 21 Johnson, E.O., and P.N. Soucacos. 2008. Nerve repair: experimental and clinical evaluation of  
22 biodegradable artificial nerve guides. *Injury*. 39 Suppl 3:S30-36.
- 23 Kanungo, B.P., E. Silva, K. Van Vliet, and L.J. Gibson. 2008. Characterization of mineralized collagen-  
24 glycosaminoglycan scaffolds for bone regeneration. *Acta Biomater*. 4:490-503.
- 25 Kehoe, S., X.F. Zhang, and D. Boyd. 2012. FDA approved guidance conduits and wraps for peripheral  
26 nerve injury: A review of materials and efficacy. *Injury-International Journal of the Care of the*  
27 *Injured*. 43:553-572.
- 28 Ki, C.S., D.H. Baek, K.D. Gang, K.H. Lee, I.C. Um, and Y.H. Park. 2005. Characterization of gelatin nanofiber  
29 prepared from gelatin-formic acid solution. *Polymer*. 46:5094-5102.
- 30 Kim, H.W., J.H. Song, and H.E. Kim. 2005. Nanoriber generation of gelatin-hydroxyapatite biomimetics for  
31 guided tissue regeneration. *Adv Funct Mater*. 15:1988-1994.
- 32 Kokai, L.E., Y.C. Lin, N.M. Oyster, and K.G. Marra. 2009. Diffusion of soluble factors through degradable  
33 polymer nerve guides: Controlling manufacturing parameters. *Acta Biomater*. 5:2540-2550.
- 34 Lee, S.K., and S.W. Wolfe. 2000. Peripheral nerve injury and repair. *J Am Acad Orthop Surg*. 8:243-252.
- 35 Leong, K.F., C.M. Cheah, and C.K. Chua. 2003. Solid freeform fabrication of three-dimensional scaffolds  
36 for engineering replacement tissues and organs. *Biomaterials*. 24:2363-2378.
- 37 Lim, S.H., X.Y. Liu, H.J. Song, K.J. Yarema, and H.Q. Mao. 2010. The effect of nanofiber-guided cell  
38 alignment on the preferential differentiation of neural stem cells. *Biomaterials*. 31:9031-9039.
- 39 Lin, Y.C., and K.G. Marra. 2012. Injectable systems and implantable conduits for peripheral nerve repair.  
40 *Biomed Mater*. 7:024102.
- 41 Lu, C.M., C.J. Chang, C.M. Tang, H.C. Lin, S.C. Hsieh, B.S. Liu, and W.C. Huang. 2009. Effects of Asymmetric  
42 Polycaprolactone Discs on Co-culture Nerve Conduit Model. *J Med Biol Eng*. 29:76-82.
- 43 Lyons, J.G., L.M. Geever, M.J. Nugent, J.E. Kennedy, and C.L. Higginbotham. 2009. Development and  
44 characterisation of an agar--polyvinyl alcohol blend hydrogel. *J Mech Behav Biomed*. 2:485-493.
- 45 Mackinnon, S.E., A.L. Dellon, A.R. Hudson, and D.A. Hunter. 1984. Chronic Nerve Compression - an  
46 Experimental-Model in the Rat. *Ann Plast Surg*. 13:112-120.
- 47 Madison, R., C.F. Dasilva, P. Dikkes, T.H. Chiu, and R.L. Sidman. 1985. Increased Rate of Peripheral-Nerve  
48 Regeneration Using Bioresorbable Nerve Guides and a Laminin-Containing Gel. *Exp Neurol*.  
49 88:767-772.
- 50 Mahoney, M.J., and K.S. Anseth. 2006. Three-dimensional growth and function of neural tissue in  
51 degradable polyethylene glycol hydrogels. *Biomaterials*. 27:2265-2274.
- 52 Marquardt, L.M., and S.E. Sakiyama-Elbert. 2013. Engineering peripheral nerve repair. *Curr Opin*  
53 *Biotechnol*. 24:887-892.

- 1 Martens, P.J., S.J. Bryant, and K.S. Anseth. 2003. Tailoring the degradation of hydrogels formed from  
2 multivinyl poly(ethylene glycol) and poly(vinyl alcohol) macromers for cartilage tissue  
3 engineering. *Biomacromolecules*. 4:283-292.
- 4 Matsumoto, K., K. Ohnishi, T. Kiyotani, T. Sekine, H. Ueda, T. Nakamura, K. Endo, and Y. Shimizu. 2000.  
5 Peripheral nerve regeneration across an 80-mm gap bridged by a polyglycolic acid (PGA)-collagen  
6 tube filled with laminin-coated collagen fibers: a histological and electrophysiological evaluation  
7 of regenerated nerves. *Brain Res*. 868:315-328.
- 8 Meek, M.F., A.S. Varejao, and S. Geuna. 2002. Muscle grafts and alternatives for nerve repair. *J Oral*  
9 *Maxillofac Surg*. 60:1095-1096; author reply 1096.
- 10 Meena, R., K. Prasad, and A.K. Siddhanta. 2007. Preparation of genipin-fixed agarose hydrogel. *J Appl*  
11 *Polym Sci*. 104:290-296.
- 12 Nafea, E.H., L.A. Poole-Warren, and P.J. Martens. 2014. Correlation of Macromolecular Permeability to  
13 Network Characteristics of Multivinyl Poly(vinyl alcohol) Hydrogels. *J Polym Sci Pol Phys*. 52:63-  
14 72.
- 15 Nakayama, K., K. Takakuda, Y. Koyama, S. Itoh, W. Wang, T. Mukai, and N. Shirahama. 2007.  
16 Enhancement of peripheral nerve regeneration using bioabsorbable polymer tubes packed with  
17 fibrin gel. *Artif Organs*. 31:500-508.
- 18 Nectow, A.R., K.G. Marra, and D.L. Kaplan. 2012. Biomaterials for the development of peripheral nerve  
19 guidance conduits. *Tissue Eng Part B Rev*. 18:40-50.
- 20 Nichols, C.M., T.M. Myckatyn, S.R. Rickman, I.K. Fox, T. Hadlock, and S.E. Mackinnon. 2005. Choosing the  
21 correct functional assay: a comprehensive assessment of functional tests in the rat. *Behav Brain*  
22 *Res*. 163:143-158.
- 23 Novajra, G., C. Tonda-Turo, C. Vitale-Brovarone, G. Ciardelli, S. Geuna, and S. Raimondo. 2014. Novel  
24 systems for tailored neurotrophic factor release based on hydrogel and resorbable glass hollow  
25 fibers. *Mater Sci Eng C Mater Biol Appl*. 36:25-32.
- 26 Oh, S.H., J.H. Kim, K.S. Song, B.H. Jeon, J.H. Yoon, T.B. Seo, U. Narnung, I.W. Lee, and J.H. Lee. 2008.  
27 Peripheral nerve regeneration within an asymmetrically porous PLGA/Pluronic F127 nerve guide  
28 conduit. *Biomaterials*. 29:1601-1609.
- 29 Okamoto, H., K.I. Hata, H. Kagami, K. Okada, Y. Ito, Y. Narita, H. Hirata, I. Sekiya, T. Otsuka, and M. Ueda.  
30 2010. Recovery process of sciatic nerve defect with novel bioabsorbable collagen tubes packed  
31 with collagen filaments in dogs. *Journal of Biomedical Materials Research Part A*. 92A:859-868.
- 32 Oliveira, J.T., R.E. Bittencourt-Navarrete, F.M. de Almeida, C. Tonda-Turo, A.M. Martinez, and J.G. Franca.  
33 2014. Enhancement of median nerve regeneration by mesenchymal stem cells engraftment in an  
34 absorbable conduit: improvement of peripheral nerve morphology with enlargement of  
35 somatosensory cortical representation. *Front Neuroanat*. 8:111.
- 36 Panseri, S., C. Cunha, J. Lowery, U. Del Carro, F. Taraballi, S. Amadio, A. Vescovi, and F. Gelain. 2008.  
37 Electrospun micro- and nanofiber tubes for functional nervous regeneration in sciatic nerve  
38 transections. *BMC Biotechnol*. 8:39.
- 39 Pfister, L.A., M. Papaloizos, H.P. Merkle, and B. Gander. 2007a. Hydrogel nerve conduits produced from  
40 alginate/chitosan complexes. *Journal of Biomedical Materials Research Part A*. 80A:932-937.
- 41 Pfister, L.A., M. Papaloizos, H.P. Merkle, and B. Gander. 2007b. Nerve conduits and growth factor  
42 delivery in peripheral nerve repair. *J Peripher Nerv Syst*. 12:65-82.
- 43 Phinney, D.G., and I. Isakova. 2005. Plasticity and therapeutic potential of mesenchymal stem cells in the  
44 nervous system. *Curr Pharm Des*. 11:1255-1265.
- 45 Prabhakaran, M.P., J.R. Venugopal, and S. Ramakrishna. 2009. Mesenchymal stem cell differentiation to  
46 neuronal cells on electrospun nanofibrous substrates for nerve tissue engineering. *Biomaterials*.  
47 30:4996-5003.
- 48 Radulescu, D., S. Dhar, C.M. Young, D.W. Taylor, H.J. Trost, D.J. Hayes, and G.R. Evans. 2007. Tissue  
49 engineering scaffolds for nerve regeneration manufactured by ink-jet technology. *Mat Sci Eng C-  
50 Bio S*. 27:534-539.
- 51 Ritfeld, G.J., B.M. Rauck, T.L. Novosat, D. Park, P. Patel, R.A.C. Roos, Y.D. Wang, and M. Oudega. 2014.  
52 The effect of a polyurethane-based reverse thermal gel on bone marrow stromal cell transplant  
53 survival and spinal cord repair. *Biomaterials*. 35:1924-1931.

- 1 Rodriguez, F.J., N. Gomez, G. Perego, and X. Navarro. 1999. Highly permeable polylactide-caprolactone  
2 nerve guides enhance peripheral nerve regeneration through long gaps. *Biomaterials*. 20:1489-  
3 1500.
- 4 Sakiyama, S.E., J.C. Schense, and J.A. Hubbell. 1999. Incorporation of heparin-binding peptides into fibrin  
5 gels enhances neurite extension: an example of designer matrices in tissue engineering. *Faseb*  
6 *Journal*. 13:2214-2224.
- 7 Sarazin, P., X. Roy, and B.D. Favis. 2004. Controlled preparation and properties of porous poly(L-lactide)  
8 obtained from a co-continuous blend of two biodegradable polymers. *Biomaterials*. 25:5965-  
9 5978.
- 10 Schmidt, C.E., and J.B. Leach. 2003. Neural tissue engineering: strategies for repair and regeneration.  
11 *Annu Rev Biomed Eng*. 5:293-347.
- 12 Schultz, S.G., and A.K. Solomon. 1961. Determination of the effective hydrodynamic radii of small  
13 molecules by viscometry. *J Gen Physiol*. 44:1189-1199.
- 14 Scuteri, A., M. Miloso, D. Foudah, M. Orciani, G. Cavaletti, and G. Tredici. 2011. Mesenchymal stem cells  
15 neuronal differentiation ability: a real perspective for nervous system repair? *Curr Stem Cell Res*  
16 *Ther*. 6:82-92.
- 17 Seckel, B.R., D. Jones, K.J. Hekimian, K.K. Wang, D.P. Chakalis, and P.D. Costas. 1995. Hyaluronic acid  
18 through a new injectable nerve guide delivery system enhances peripheral nerve regeneration in  
19 the rat. *J Neurosci Res*. 40:318-324.
- 20 Sill, T.J., and H.A. von Recum. 2008. Electrospinning: applications in drug delivery and tissue engineering.  
21 *Biomaterials*. 29:1989-2006.
- 22 Song, J.H., H.E. Kim, and H.W. Kim. 2008. Production of electrospun gelatin nanofiber by water-based co-  
23 solvent approach. *J Mater Sci-Mater M*. 19:95-102.
- 24 Stokols, S., and M.H. Tuszynski. 2004. The fabrication and characterization of linearly oriented nerve  
25 guidance scaffolds for spinal cord injury. *Biomaterials*. 25:5839-5846.
- 26 Subramanian, A., U.M. Krishnan, and S. Sethuraman. 2012. Fabrication, Characterization and In Vitro  
27 Evaluation of Aligned PLGA-PCL Nanofibers for Neural Regeneration. *Ann Biomed Eng*. 40:2098-  
28 2110.
- 29 Sun, C., X. Jin, J.M. Holzwarth, X. Liu, J. Hu, M.J. Gupte, Y. Zhao, and P.X. Ma. 2012. Development of  
30 channeled nanofibrous scaffolds for oriented tissue engineering. *Macromol Biosci*. 12:761-769.
- 31 Sundback, C., T. Hadlock, M. Cheney, and J. Vacanti. 2003. Manufacture of porous polymer nerve  
32 conduits by a novel low-pressure injection molding process. *Biomaterials*. 24:819-830.
- 33 Sunderland, S. 1951. A classification of peripheral nerve injuries producing loss of function. *Brain : a*  
34 *journal of neurology*. 74:491-516.
- 35 Suri, S., and C.E. Schmidt. 2010. Cell-Laden Hydrogel Constructs of Hyaluronic Acid, Collagen, and Laminin  
36 for Neural Tissue Engineering. *Tissue Eng Pt A*. 16:1703-1716.
- 37 Taras, J.S., and S.M. Jacoby. 2008. Repair of lacerated peripheral nerves with nerve conduits. *Tech Hand*  
38 *Up Extrem Surg*. 12:100-106.
- 39 Teo, W.E., M. Kotaki, X.M. Mo, and S. Ramakrishna. 2005. Porous tubular structures with controlled fibre  
40 orientation using a modified electrospinning method. *Nanotechnology*. 16:918-924.
- 41 Teo, W.E., and S. Ramakrishna. 2005. Electrospun fibre bundle made of aligned nanofibres over two fixed  
42 points. *Nanotechnology*. 16:1878-1884.
- 43 Thompson, D.M., and H.M. Buettner. 2001. Schwann cell response to micropatterned laminin surfaces.  
44 *Tissue Eng*. 7:247-265.
- 45 Timnak, A., F.Y. Gharebaghi, R.P. Shariati, S.H. Bahrami, S. Javadian, S.H. Emami, and M.A. Shokrgozar.  
46 2011. Fabrication of nano-structured electrospun collagen scaffold intended for nerve tissue  
47 engineering. *J Mater Sci-Mater M*. 22:1555-1567.
- 48 Tonda-Turo, C., C. Audisio, S. Gnani, V. Chiono, P. Gentile, S. Raimondo, S. Geuna, I. Perroteau, and G.  
49 Ciardelli. 2011a. Porous Poly(epsilon-caprolactone) Nerve Guide Filled with Porous Gelatin Matrix  
50 for Nerve Tissue Engineering. *Adv Eng Mater*. 13:B151-B164.
- 51 Tonda-Turo, C., E. Cipriani, S. Gnani, V. Chiono, C. Mattu, P. Gentile, I. Perroteau, M. Zanetti, and G.  
52 Ciardelli. 2013. Cross linked gelatin nanofibres: Preparation, characterisation and in vitro studies  
53 using glial-like cells. *Mat Sci Eng C-Mater*. 33:2723-2735.

- 1 Tonda-Turo, C., P. Gentile, S. Saracino, V. Chiono, V.K. Nandagiri, G. Muzio, R.A. Canuto, and G. Ciardelli.  
2 2011b. Comparative analysis of gelatin scaffolds crosslinked by genipin and silane coupling agent.  
3 *Int J Biol Macromol.* 49:700-706.
- 4 Vleggeert-Lankamp, C.L.A.M., G.C.W. de Ruyter, J.F.C. Wolfs, A.P. Pego, R.J. van den Berg, H.K.P.  
5 Feirabend, M.J.A. Malessy, and E.A.J.F. Lakke. 2007. Pores in synthetic nerve conduits are  
6 beneficial to regeneration. *Journal of Biomedical Materials Research Part A.* 80A:965-982.
- 7 Wang, W., S. Itoh, A. Matsuda, S. Ichinose, K. Shinomiya, Y. Hata, and J. Tanaka. 2008. Influences of  
8 mechanical properties and permeability on chitosan nano/microfiber mesh tubes as a scaffold for  
9 nerve regeneration. *Journal of Biomedical Materials Research Part A.* 84A:557-566.
- 10 Wang, X.D., W. Hu, Y. Cao, J. Yao, J. Wu, and X.S. Gu. 2005. Dog sciatic nerve regeneration across a 30-  
11 mm defect bridged by a chitosan/PGA artificial nerve graft. *Brain.* 128:1897-1910.
- 12 Wang, Y.S., C.W. Zhou, M. Yao, Y. Li, Y.G. Liu, and W. Zheng. 2012. Biodegradable parallel and porous  
13 HSPG/collagen scaffolds for the in vitro culture of NSCs for the spinal cord tissue engineering. *J*  
14 *Porous Mat.* 19:173-180.
- 15 Wen, X.J., and P.A. Tresco. 2006. Fabrication and characterization of permeable degradable poly(DL-  
16 lactide-co-glycolide) (PLGA) hollow fiber phase inversion membranes for use as nerve tract  
17 guidance channels. *Biomaterials.* 27:3800-3809.
- 18 Wiberg, M., and G. Terenghi. 2003. Will it be possible to produce peripheral nerves? *Surg Technol Int.*  
19 11:303-310.
- 20 Widmer, M.S., P.K. Gupta, L.C. Lu, R.K. Meszlenyi, G.R.D. Evans, K. Brandt, T. Savel, A. Gurlek, C.W.  
21 Patrick, and A.G. Mikos. 1998. Manufacture of porous biodegradable polymer conduits by an  
22 extrusion process for guided tissue regeneration. *Biomaterials.* 19:1945-1955.
- 23 Williams, L.R., N. Danielsen, H. Muller, and S. Varon. 1987. Exogenous Matrix Precursors Promote  
24 Functional Nerve Regeneration across a 15-Mm Gap within a Silicone Chamber in the Rat. *J Comp*  
25 *Neurol.* 264:284-290.
- 26 Wong, J.Y., J.B. Leach, and X.Q. Brown. 2004. Balance of chemistry, topography, and mechanics at the  
27 cell-biomaterial interface: Issues and challenges for assessing the role of substrate mechanics on  
28 cell response. *Surf Sci.* 570:119-133.
- 29 Xie, J., M.R. MacEwan, A.G. Schwartz, and Y. Xia. 2010. Electrospun nanofibers for neural tissue  
30 engineering. *Nanoscale.* 2:35-44.
- 31 Xu, H.X., Y.H. Yan, and S.P. Li. 2011. PDLLA/chondroitin sulfate/chitosan/NGF conduits for peripheral  
32 nerve regeneration. *Biomaterials.* 32:4506-4516.
- 33 Yamada, A., F. Niikura, and K. Ikuta. 2008. A three-dimensional microfabrication system for  
34 biodegradable polymers with high resolution and biocompatibility. *J Micromech Microeng.* 18.
- 35 Yannas, I.V., M. Zhang, and M.H. Spilker. 2007. Standardized criterion to analyze and directly compare  
36 various materials and models for peripheral nerve regeneration. *J Biomat Sci-Polym E.* 18:943-  
37 966.
- 38 Yucel, D., G.T. Kose, and V. Hasirci. 2010. Polyester based nerve guidance conduit design. *Biomaterials.*  
39 31:1596-1603.
- 40 Zeugolis, D.I., S.T. Khew, E.S.Y. Yew, A.K. Ekaputra, Y.W. Tong, L.Y.L. Yung, D.W. Hutmacher, C. Sheppard,  
41 and M. Raghunath. 2008. Electro-spinning of pure collagen nano-fibres - Just an expensive way to  
42 make gelatin? *Biomaterials.* 29:2293-2305.
- 43 Zhu, Y., A. Wang, S. Patel, K. Kurpinski, E. Diao, X. Bao, G. Kwong, W. Young, and S. Li. 2011. Engineering  
44 Bi-layer Nanofibrous Conduits for Peripheral Nerve Regeneration. *Tissue Eng Part C Methods.*

45

46